APPENDIX A: Mechanical Loads

This page is intentionally blank

APPENDIX A

Mechanical Loads

A.1 Purpose

While conducting the dry cask storage PRA, specific questions were identified that related to the handling, transfer, and storage of the cask system and the effects of natural phenomena such as wind, flood, and earthquake. This Appendix contains summaries of the results and corresponding calculations to address each of those questions.

The purpose of this Appendix is to examine several initiating events during the handling, transfer, and storage of the cask system and to determine the effects of natural phenomena (wind, flood, and earthquake). The results of this evaluation will provide the stresses in the multi-purpose canister (MPC), which contains the spent fuel that will be used in subsequent evaluations to determine the probability of breaching the MPC.

A.2 Scope

The scope of this evaluation is limited to performing calculations in response to specific questions. These questions all relate to the transfer cask and the storage cask used at the subject plant. The questions are as follows:

Handling Phase Questions

1. If the fuel handling building crane is traveling at maximum speeds (Bridge 15 m/min (50 ft/min), Trolley 3 m/min (10 ft/min), and Hoist 1.3 m/min (4.2 ft/min)) with an MPC and its lid secured by gravity in the transfer overpack, what drop height causes the transfer cask to tip-over onto the concrete floor?
2. Same question as Question 1 but the MPC lid is "sealed."
3. Analyze the vertical drop of the transfer cask containing a sealed MPC falling on the concrete floor at ground elevation from heights of 1.5, 12.2, 21.3, and 30.5 meters (5, 40, 70, and 100 feet). Determine the magnitude and location of maximum stresses/strains in the MPC.
4. Analyze the vertical drop of the transfer cask containing a sealed MPC falling onto the storage overpack at ground elevation from heights of 1.5, 12.2, and 24.4 meters (5, 40, and 80 ft). Determine the magnitude and location of maximum stresses/strains in the MPC.
5. Determine the magnitude and location of maximum stresses/strains in the MPC when a sealed MPC falls vertically 5.8 m (19 ft) into the storage overpack.

Transfer Phase Question Topics

6. If the storage cask drops onto the Independent Spent Fuel Storage Installation (ISFSI) concrete pad, asphalt area, or gravel area, while it is hung from the top trunnion and being transported by the crawler, will it slide and/or tip-over? If tip-over can occur, what velocity of the crawler would be required to tip it over? How much time does the operator have to stop the crawler before tip-over occurs? What are the stresses in the MPC?
7. If the crawler vehicle weighing 71,440 kg (157,500 lb) is traveling at 0.64 km/h (0.4 mi/h) while carrying the storage cask weighing 163,293 kg (360,000 lb) and hits another storage cask on a concrete pad, will the impact cause the struck cask to slide or tip-over?

(A) If it slides, will a sliding storage cask hit another storage cask? If it hits another storage cask, what are the maximum stresses in the MPC?

(B) If it tips over, what are the maximum stresses in the MPC?

(C) If it does not slide or tip-over, what travel velocity of the crawler would be necessary to strike the storage cask and cause it to slide and/or tip-over?

Storage Phase Question Topics

8. What seismic forces will cause the storage cask to slide and/or tip-over?
9. What impact forces due to a given small aircraft, tornado missiles (beyond design basis) and heavy objects in flood waters will cause the storage cask to slide and/or tip-over? If the impacting object penetrates the storage overpack, what will be the stresses in the MPC?
10. If the storage cask tips over on the concrete pad, what will be the stresses in the MPC?
11. If the storage cask tips over, will the impact of the cask tipping over on another storage cask or on the concrete pad cause the overpack lid to be dislodged such that the MPC could slide out?
12. Will the structural integrity of the cask system be jeopardized by shock waves caused by postulated explosions? If not, provide the supporting arguments.

A.3 Method

To evaluate the structural response of the cask system to the event scenarios posed by the twelve questions, several methods of analysis were used, which included hand calculations based on first principles, common analytical methods and industry recognized approaches, and solution of the differential equations of motion for which closed form solutions were obtained. Wherever possible existing analyses, such as the Holtec finite element analysis of the MPC, fuel basket and fuel basket supports (Reference A.1), that had been performed for a number of impact events were utilized by scaling the stress results in Reference A.1 by the ratio of the maximum acceleration calculated in response to the question divided by the acceleration in Reference A.1. For the cask drop impact scenarios, the Holtec finite element models were modified and expanded, as discussed in the appropriate sections below.

A.4 Calculation Summary Descriptions

A.4.1 Question 1

If the fuel handling building crane is traveling at maximum speeds (Bridge 15 m/min (50 ft/min), Trolley 3 m/min (10 ft/min), and Hoist 1.3 m/min (4.2 ft/min)) with an MPC and its lid secured by gravity in the transfer overpack, what drop height causes the transfer cask to tip-over onto the concrete floor?

A.4.2 Question 2

Same as Question 1 but the MPC lid is “sealed.”

The response to Questions 1 and 2 are combined into one evaluation. Solutions are obtained for various cask orientations when it is dropped. When the transfer cask impacts the concrete floor it is assumed to have the same orientation and horizontal velocity as when it was dropped. The vertical velocity is increased (positive measured down) by the velocity added during free fall. At impact the horizontal and vertical velocity components are transferred to an equivalent rotational velocity. The transfer cask then rotates about the point of impact until it either tips over (when the center of gravity intersects a vertical line immediately above the point of impact) or rotates back to a vertical orientation. The question is

resolved by determining the rotational velocity needed to tip-over the transfer cask. It should be noted that the transfer cask drops at an acceleration of 1 g so that the lid secured by gravity would not separate from the MPC during the fall. The answers to Questions 1 and 2 are therefore the same. Detailed analyses are first summarized and then followed by a discussion of the answer.

<u>With No Initial Velocity</u>

The specific geometry of the transfer cask is shown in Figure A.1. The weight of the loaded transfer cask is assumed to be 86,636 kg (191,000 lb) but as will be seen the weight does not enter into the solution. Note that the transfer cask is dropped at an angle (α) with the vertical and the drop height to the center on the base of the cask is H. When the angle (α) equals 90 - Φ = 67°, the transfer cask is oriented so that the center of gravity of the cask is located above the point on the cask that first impacts the slab. It is obvious that the transfer cask will tip-over if it is dropped at angles less than 67°.

Figure A.1. Geometry of Transfer Cask

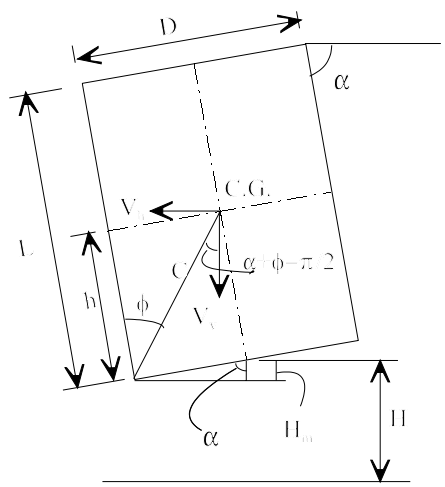

Note that it is not possible to drop the transfer cask at angles smaller than α = 67° unless the drop height (H_m) is greater than that calculated from the expression:

$$\text{Cos}\ \alpha = \frac{H_m}{D/2} \qquad \text{(A.1)}$$

where:

D	=	2.06 m (81.25 inches)
L	=	4.84 m (190.5 inches)
h	=	2.39 m (93.95 inches)
C	=	2.64 m (104 inches)
Φ	=	23°
H_m	=	½ * D * Cos α

Therefore, with no initial velocity a tip-over will occur only if the drop height is greater than 40 cm (15.9 inches) and the angle α is less than 67°.

<u>With Initial Velocity</u>

At impact the horizontal (V_h) and vertical (V_v) velocities of the cask are transformed to a rotational velocity of the transfer cask (θ_o'):

The subsequent response of the transfer cask is developed next. A sketch of the transfer cask defining the response parameters used is shown in Figure A.2.

Figure A.2. Rotation of Transfer Cask after Impact

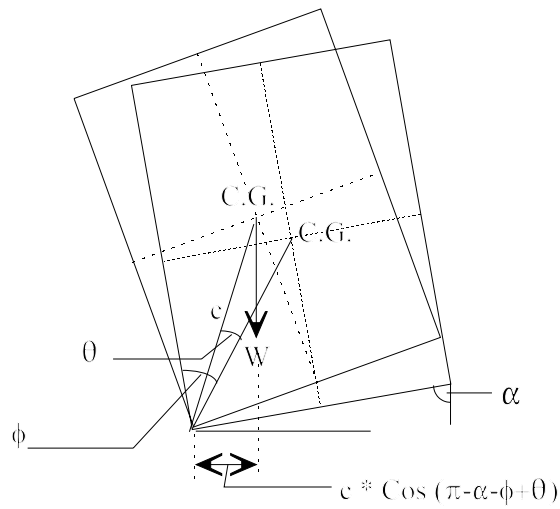

The response of the cask is then governed by:

$$\theta_0' = \frac{V_h \mathrm{Sin}\left(\pi - \phi - \alpha\right) - V_v \mathrm{Sin}\left(\phi + \alpha - \pi/2\right)}{C} \qquad (A.2)$$

$$J\theta'' + W\ C\ \ \mathrm{Cos}\left(\pi - \phi - \alpha + \theta\right) = 0 \qquad (A.3)$$

with the initial conditions, $\theta(0) = 0$; and $\theta'(0) = \theta_o'$ and where J is the rotational inertia of the transfer cask.

It is interesting to examine this family of equations before discussing their solution. Equation A.2 demonstrates that the vertical velocity reduces the rotational velocity imparted to the transfer cask at impact. It can therefore be concluded that any positive vertical velocity decreases the possibility that the transfer cask will tip-over.

Due to free fall the upward initial velocity 1.3 m/min (4.2 ft/min) caused by the hoist is reduced to zero at some drop height. A solution is therefore sought where the vertical velocity is zero at impact. This

solution can be found simply by equating the kinetic energy (KE) of the transfer cask at impact to the potential energy (PE) developed as the center of gravity is raised to a point where it is directly over the point of impact. The kinetic energy is:

$$KE = \frac{WV_h^2}{2g} \qquad (A.4)$$

The potential energy when the center of gravity is over the point of rotation is:

$$PE = W\,C\left[1 - \mathrm{Cos}\left(\phi - \frac{\pi}{2} + \alpha\right)\right] \qquad (A.5)$$

Equating the two;

$$V_h = \left\{2\,g\,C\left[1 - \mathrm{Cos}\left(\phi - \frac{\pi}{2} + \alpha\right)\right]\right\}^{1/2} \qquad (A.6)$$

The maximum horizontal velocity is $(50^2 + 10^2)^{1/2} = 51$ ft/min and Equation A.6 shows that at this velocity the transfer cask will tip-over only when the angle $\alpha < 70°$. If the horizontal velocity is zero the solution to Equation A.6 shows that the transfer cask will tip-over when the angle $\alpha < \pi/2 - \Phi = 67°$. The fact that these two solutions are so close indicates that the horizontal velocities imparted to the transfer cask by the crane are very small and have little effect on the problem. It is also interesting to note that the height of the drop is not involved in the solution. In effect it has been assumed that the vertical velocity is zero which can only occur for very low drop heights. Any higher drops would reduce the solution $\alpha = 70°$ but it cannot be reduced further than 67°.

In summary the velocities imparted by the crane are very small and have little effect on the conditions required for the transfer cask to tip-over. The solutions indicate that, for the given crane velocities, the transfer cask will tip-over only if it is dropped at an angle such that the center of gravity of the cask is over the point of first contact with the floor. This angle requires that the transfer cask axis be oriented less than 67° with the horizontal. This can only occur when the drop height of the transfer cask is greater than 40 cm (15.9 inches).

A.4.3. Question 3

Analyze the vertical drop of the transfer cask containing a sealed MPC falling on the concrete floor at ground elevation from heights of 1.5, 12.2, 21.3, and 30.5 meters (5, 40, 70, and 100 feet). Determine the magnitude and location of maximum stresses/strains in the MPC.

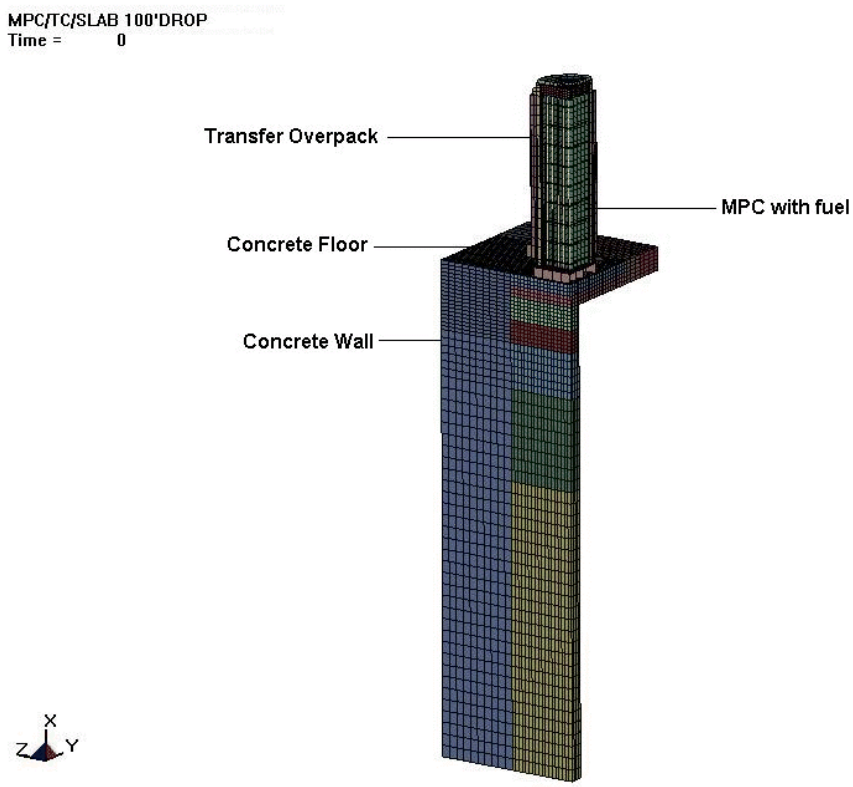

Figure A.3. Transfer Cask Vertical Drop onto Concrete Floor/wall Finite Element Model

Model Development

To respond to this question, a finite element model was developed that includes the MPC, fuel assemblies, fuel basket, fuel basket supports, transfer overpack, and concrete floor and wall (Reference A.24). These components are shown in Figures A.3 through A.5. The finite element model (FEM) shown in Figure A.3 contains all of the structural components mentioned above. The model is a quarter-model representation of the cask system and concrete floor/wall, which takes advantage of symmetry about two orthogonal vertical planes through the centerline of the MPC.

Figure A.4 shows a close-up view of the Transfer Overpack (TO) and MPC resting on the concrete floor, and Figure A.5 shows another close-up view at the MPC connection to the MPC base plate along one plane of symmetry. The fuel basket plate on the plane of symmetry has been removed so that the fuel assemblies within the basket compartments can be seen.

The TO model used in this analytical study is the 125 ton HI-TRAC Model with the MPC-68 canister (full of fuel) and bottom transfer lid, as received from HOLTEC International. The major revisions made are as follows (A complete listing of changes can be found in Reference A.24.):

1. To minimize the significant computational effort, a quarter model representation of the TO, MPC, and concrete floor/wall beneath the floor was developed. This quarter model was created considering the two vertical planes of symmetry that exist for the TO and the MPC. The TO quarter model was developed from the HOLTEC half model by deleting half of the nodes and element definitions and creating a node set to define the two planes of symmetry.

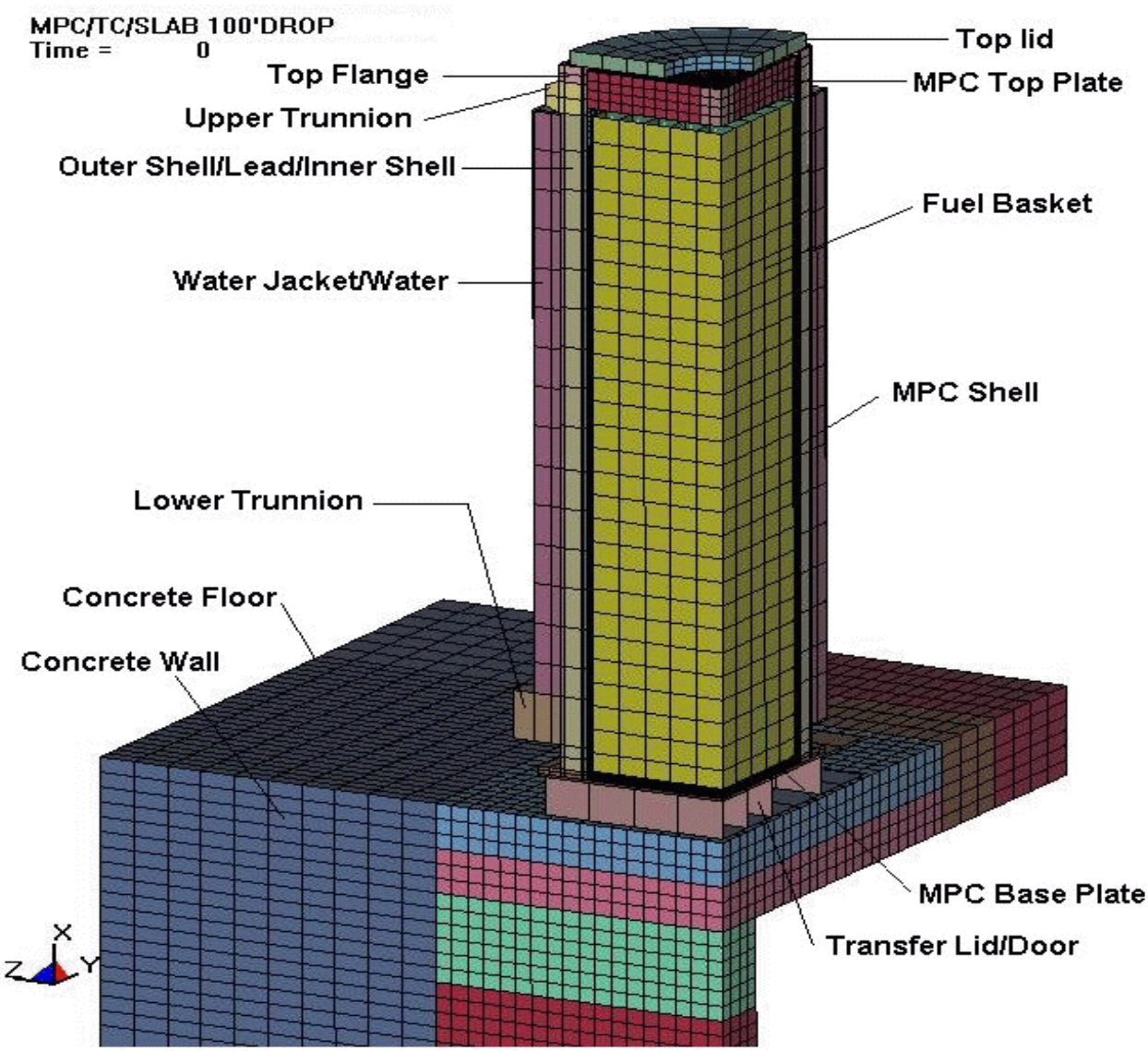

Figure A.4. Transfer Cask Vertical Drop onto Concrete Floor/wall. Close-up View of the Cask Resting on the Concrete Floor.

2. Contact surfaces within various components of the TO and between the TO and the concrete floor were defined to properly transfer impact forces.

3. The HOLTEC TO model represents the combined MPC/fuel region modeled as brick type finite elements. This single brick representation of the MPC/fuel was deleted and replaced by a detailed finite element model of the MPC and internal components, as described later. (Removal of the single brick representation of the fuel and basket and replacing it with an explicit representation of the fuel and basket is not necessary for the analysis of the MPC. This was only done in the event that the model would be used to predict fuel cladding strains.)

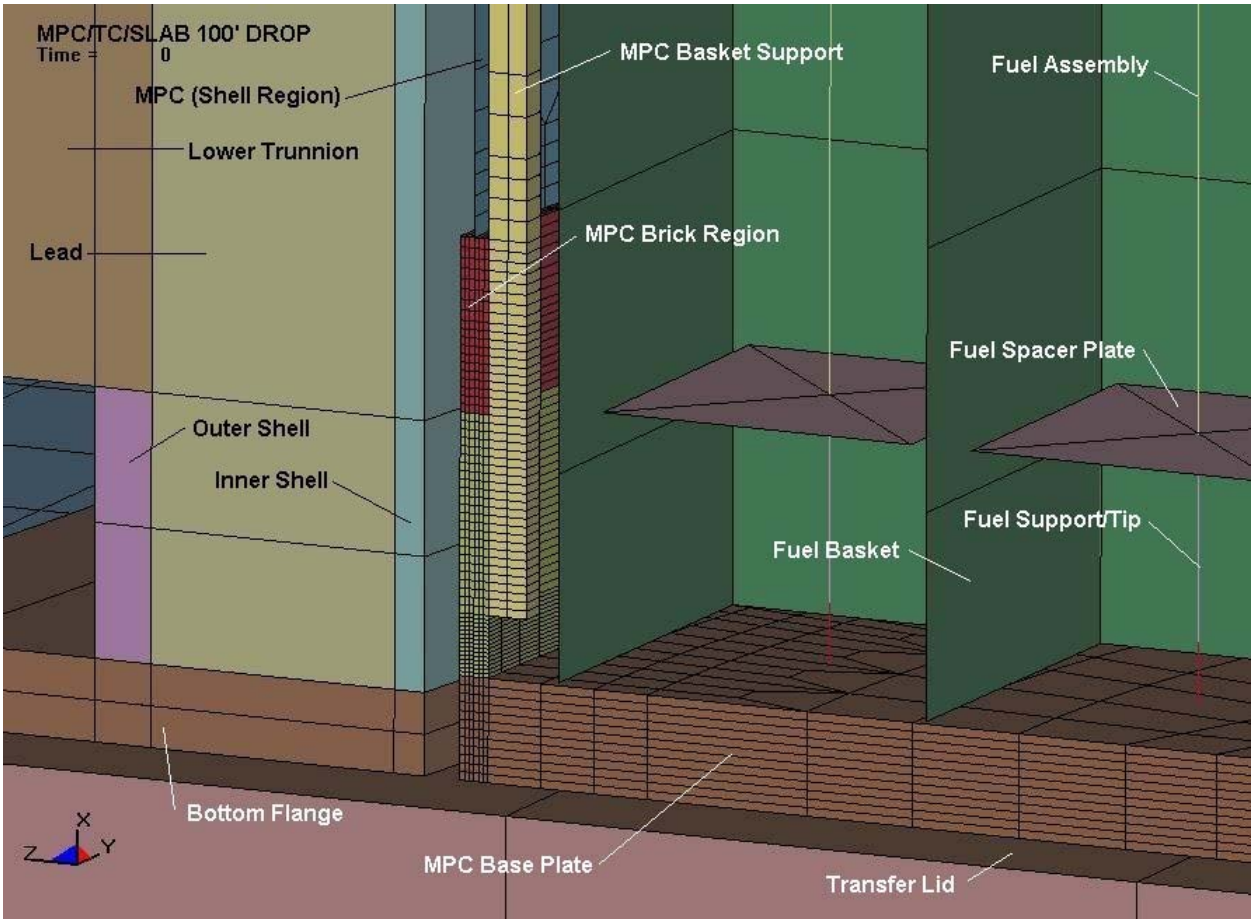

Figure A.5. Transfer Cask Vertical Drop onto Concrete Floor/wall Showing MPC Connection to the MPC Base Plate at Plane of Symmetry, Time = 0

The dynamic impact analyses were performed using the LS-DYNA computer code, Version 970, Rev. 3858 (Reference A.4). LS-DYNA is a general-purpose finite element code for analyzing the large deformation dynamic response of structures. The computer code utilizes an explicit solution method to solve for the dynamic impact response. Strains in all elements are calculated at each time step, and if the effective plastic strain reaches the user specified failure strain for a particular element, that element is automatically eliminated from the model and the analysis continues.

The material model for the Type 304 stainless steel components in the TO and MPC are based on a bilinear elastic plastic stress strain curve, which requires the elastic modulus, yield strength, tangent modulus, and failure strain as input. The modulus of elasticity was taken from the ASME Code, Division 1 - Appendices (Reference A.5). The material properties for the yield strength and ultimate strength were based on the data contained in Appendix B, and then adjusted for strain rate effects using the information in Reference A.6. The engineering strain at failure was based on the data contained in Reference A.6 at a high strain rate. The tangent modulus was calculated from the yield strength, ultimate strength and engineering failure strain. All of these material properties were developed at the appropriate temperature for each component of the TO and MPC.

The design temperatures for the various TO and MPC components are presented in Table A.1, and are consistent with HOLTEC's design (Reference A.1). The material properties (modulus of elasticity, yield

strength, tangent modulus, and rupture strain) at the temperatures of the TO and MPC components are presented in Table A.2.

Table A.1. Transfer Overpack, MPC, and Fuel Cladding Temperatures

Components	**Temperature °C (°F)**
Fuel and fuel basket	393 (740)
MPC Shell	237 (459)
Transfer overpack inner shell and water jacket inner surface	162 (323)
Water jacket outer surface	106 (223)
Top lid, transfer lid, trunnion, water jacket ribs, water, and transfer lid vertical plates	162 (323)

Table A.2: Material Properties

Material	Temp °C (°F)	Modulus of Elasticity (psi)	Yield Strength (psi)	Tangent Modulus (psi)	Engineering Strain at Failure (in/in)	Minimum True Strain at Failure (1) (in/in)
Stainless Steel (Type 304)	393 (740)	2.35×10^{7}	23,386	1.03×10^{5}	0.377	0.92
	237 (459)	2.61×10^{7}	38,344	5.85×10^{4}	0.456	0.92
	162 (323)	2.69×10^{7}	44,719	4.60×10^{4}	0.480	0.92
	106 (223)	2.75×10^{7}	51,012	4.03×10^{4}	0.498	0.92
Zircaloy-2	393 (740)	9.80×10^{6}	43,807	1.41×10^{5}	NA	NA
Lead	162 (323)	1.90×10^{6}	380	0.0	NA	NA

1 psi = 6.895 kPa
(1) Includes the effects of strain rate and temperature up to 100/sec and 1000F respectively.

Although stainless steel material Types 304LN, 316, and 316LN might also be used to construct the TO, MPC and other stainless steel components, the material properties (yield and ultimate strength) for stainless steel Type 304 are equal to or less (i.e., more conservative) than the values for Type 304LN, 316, and 316LN for the temperature range of interest, and therefore were used in the analysis.

The material model used in the analysis assumes that the stress-strain curve and failure criterion (rupture strain), which are derived from tensile test data, are also applicable to elements in compression. Using the same stress-strain curve in tension and compression is realistic for steel materials.

Since the LS-DYNA computer program considers the reduction in the area of the finite elements in the computation of stress during the execution of the analysis, a true stress strain curve is expected to be input for the material properties. In the analyses, however, the more conservative engineering stress strain curve was used. It is well known that engineering stress strain values are very close to the true stress strain values during the initial stages of yielding, and that in the plastic region the engineering stress values are always lower than the true stress values. Thus, at any given deformation level the total energy absorbed by the MPC will be underestimated. This results in a conservative response because it overestimates the total deformation (strain). For comparison, the minimum true strain at failure of Type 304 stainless steel is also shown in Table A.2.

The MPC consists of the 1.27 cm (½ inch) thick vertical cylindrical shell, a 25.4 cm (10 inch) thick top shield plate, and a 6.35 cm (2.5 inch) thick base plate. The top plate and base plate are modeled using brick elements. The MPC cylindrical shell is modeled using six brick elements through the thickness from the top of the base plate to 30 cm (11.75 inches) above the base plate. Beyond this elevation, the vertical shell wall is modeled using shell elements. Shell elements are sufficiently accurate for the region above 30 cm (11.75 inches), and this transition to shell type elements reduces the execution time for solution. Even with this transition to shell type elements, the entire model is quite large with 79,973 nodes and 66,704 elements.

The fuel basket is modeled as a grid of 0.635 cm (¼ inch) thick vertical plates spaced 16.5 cm (6.5 inches) apart to form the square cells that hold the fuel assemblies. The fuel basket is freestanding on top of the MPC base plate. The LS-DYNA model of the fuel basket is shown in Figures A.4 and A.5. In Figure A.5, the basket plates at the plane of symmetry have been removed to show the fuel assemblies within the basket cell walls. The mass density of the basket plates was increased to account for the additional boral material attached to the sides of the basket plates. The material model used for the TO and MPC was also utilized for the stainless steel fuel basket plates. The specific material properties used for the fuel basket are shown in Tables A.1 and A.2.

To maintain a reasonable execution time, a single equivalent beam model of a typical fuel assembly was developed and placed inside each of the basket cell compartments. Each fuel assembly model consisted of a fuel support region (at the bottom of the fuel assembly), fuel region, and a handle (at the top of the fuel assembly). To capture the interaction between the fuel assemblies and the MPC base plate, it was necessary for the fuel beam to have plastic capability. To incorporate plasticity in a beam element, LS-DYNA requires that the beam be defined with explicit dimensions. To obtain the correct assembly stiffness and nonlinear behavior, the fuel region was modeled as a single circular tube with cross-sectional dimensions equal to an individual fuel rod, and the yield stress, modulus of elasticity, tangent modulus, and mass density were multiplied by the total number of fuel rods in the assembly.

In this analysis, the primary purpose of the fuel assembly model is to capture the overall effects of the fuel assembly on the structural response of the MPC in a vertical drop. Therefore, the most important parameters are the mass, vertical stiffness, and energy absorption capability of the fuel assemblies. An assumption made in the fuel assembly model is that the mass of the fuel is added to the mass of the fuel cladding, but only the fuel cladding provides stiffness. This assumption is consistent with the methodology utilized by HOLTEC in its design (Reference A.7), and complies with References A.25 and A.26.

The same material model and material properties (elastic modulus, yield strength, tangent modulus, and rupture strain) used for the fuel basket described above, were also utilized for the stainless steel fuel support (beneath the fuel region) and the handle (above the fuel region). The material properties used for the fuel region were based on the properties of Zircaloy-2 cladding material at a temperature of 483°C

(902°F) (References A.8 and A.9). Table A.2 presents the various material properties used for the fuel assembly members.

Based on calculations performed by HOLTEC (Reference A.7), the fuel region was expected to buckle elastically. However, LS-DYNA does not check for classical bifurcation buckling directly; but it can achieve an accurate prediction of static buckling by introducing a tiny bias (initial deflection) in the middle of the fuel rod. Therefore, a small bias was introduced in the middle of each equivalent fuel beam (between spacer grids) to allow large lateral deformation to take place.

Also included in the fuel assembly model are nine spacer plates (grids), at the elevations specified in the fuel assembly design drawings. The spacers, modeled with shell elements, are constrained to move vertically and horizontally with the equivalent fuel beams. A small gap is modeled between these spacer plates and the basket cell walls. Once the gap is closed, the basket cell walls provide lateral restraint for the spacer plates, which provide lateral restraint to the fuel rods. The fuel assemblies, like the fuel basket, are also freestanding on top of the MPC base plate.

A finite element model of the concrete floor and wall beneath the floor was developed. The model of the concrete wall is 12.5 m (41 ft) high from the bottom of the floor, 3.96 m (13 ft) long and 38 cm (15 inches) thick. The concrete floor is 3.96 m (13 ft) wide, 3.96 m (13 ft) long and 61 cm (24 inches) thick. This concrete floor/wall model is a quarter model representation of the actual structure and is consistent with the quarter models of the TO and MPC. Although the actual floor and wall do not have two well-defined planes of symmetry, this representation is considered reasonable.

The concrete floor/wall model was developed with 10 separate "parts" using the same concrete material model, each of which can be adjusted independently when needed for hourglass control or to change element formulation types. A finer mesh was developed near the impact region, while a coarser mesh was created away from this critical region. The concrete floor/wall has fixed boundary conditions at the ends of the wall and at the edges of the floor, excluding the two planes of symmetry.

The concrete material model and the material properties utilized in the analyses are those used by the cask manufacturer in their analyses for design certification and are presented in Appendix C of Reference A.11. A comparison analysis using an alternate concrete material model was also performed to determine whether LS-DYNA Material Model Type 16, which was used in the analysis, is reasonable and comparable to other more recently developed material models. The results indicate that the alternative material model gives comparable results to Material Model Type 16.

The transfer cask rests on top of the concrete floor at the start of the analysis, and the drop height was simulated by introducing an initial velocity corresponding to the desired drop height. The initial velocity was calculated using the expression:

$Velocity = \sqrt{2gh}$, where g is the acceleration of gravity and h is the drop height.

Four different drop heights at 1.5, 12.2, 21.3, and 30.5 meters (5, 40, 70, and 100 feet) were considered in the vertical drop analyses.

The design of the TO specified a small gap between the MPC shell wall and the inner shell of the TO. If after the fall the MPC lands at the center of the bottom lid of the TO, there would be a uniform gap equal to 0.5 cm (0.203 inches) based on average construction tolerances. Under this configuration, when the MPC shell deforms radially by an amount greater than the uniform radial gap, the TO provides resistance to further radial deformation. For the analysis reported herein, a worst-case assumption was made that

during the accidental drop of the MPC/TO, the MPC may land completely to one side of the TO. This creates a maximum gap on the opposite side equal to approximately 1.03 cm (0.406 inches) which is twice the average. This off-center drop location is simulated in the analysis by circumferentially enlarging the gap between MPC shell and TO inner shell to 1.03 cm (0.406 inches). In this manner, the analysis can provide an estimate of the effect of an off-center drop, while keeping the quarter model representation of the actual casks.

Analysis Strategy and Modifications to the Finite Element Model

The strategy behind the development of a finite element model and subsequent analysis must reflect the intended use of the results. In this case the results will ultimately be used to predict the probability of failure of the MPC confinement boundary. As such, the results from the finite element analysis must support the methodology used to predict material failure in the MPC shell and weldments.

Following receipt of the report and models (Reference A.24), the engineering failure strain limit was eliminated which had been set for the deletion of "failed" elements. This was done as a result of the a revision of the weld failure methodology in Appendix B so that the actual true strain, which is the result that is directly linked to the probability of weld failure in Appendix B, could be continuously computed until the end of the event. By running the models this also allowed to calculate the Triaxiality Factor at the location of maximum strain. As explained in Appendix B, the Triaxiality Factor is an important parameter for predicting failure, because it accounts for loss of material ductility in regions where a triaxial state of stress may constrain plastic flow.

As part of accepting the drop analysis report and input files, shakedown evaluations of the model were performed. Based on those results the following modifications were made:

1. All analyses were run using double-precision.
2. The basket supports' attachment to the MPC shell was modified to more accurately reflect the Holtec drawings.
3. The MPC base plate mesh was slightly modified at the junction with the shell to remove a local hard spot in the mesh.

These modifications were included in all analyses of the drops of the transfer cask onto the concrete floor and the 19 foot drop of the MPC into the storage overpack.

Analysis Results

The drop heights selected for analysis were 1.5, 12.2. 21.3 and 30.5 meters (5, 40, 70 and 100 feet), which provide results at the maximum drop height and at intermediate levels. The structural response of the MPC for the vertical end drop of the transfer cask onto the concrete floor are summarized in Table A.3. For each drop height, the maximum effective plastic strain (EPS) in the MPC shell, the element producing the maximum EPS and the true strain at failure are tabulated. Only the 30.5 m (100 ft) drop is discussed in detail.

Table A.3. Structural Response of the MPC for Various Drop Heights

Drop Height m (ft)	Maximum Effective Plastic Strain cm/cm (in/in)	Element Number with Maximum Effective Plastic Strain	Minimum True Strain at Failure cm/cm (in/in)
1.52 (5)	0.024	16539	0.92
12.2 (40)	0.195	15973	0.92
21.3 (70)	0.240	15997	0.92
30.5 (100)	0.256	15997	0.92

Figures A.6 and A.7 show the deformation of the MPC shell and basket supports for the 30.5 m (100 ft) drop case at the end of the event (0.022 seconds) when the kinetic energy has reached a minimum and the transfer overpack and MPC begin rebounding from the impact. These figures show the response of the structural components at the connection of the MPC cylindrical shell to the base plate adjacent to the plane of symmetry through the center of the concrete wall. They clearly show that the deformation is dominated by buckling in the lower region of the shell. The figures also show that the MPC shell wall deforms primarily in a vertical downward direction, and radially outward near the base plate. In addition, Figure A.7 shows that there is some rotation of the MPC base plate at the junction with the shell wall. This helps relieve some of the strain in the shell at this intersection location.

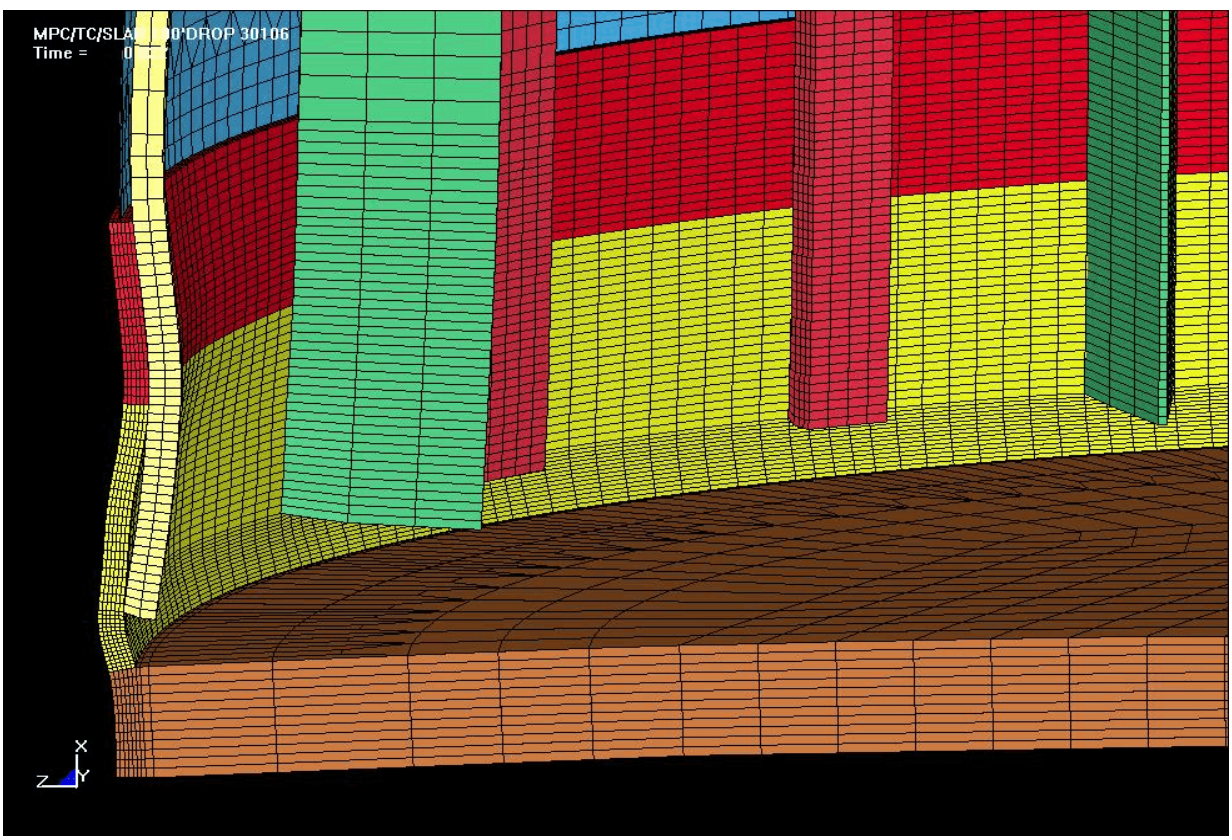

Figure A.6. Deformation of the MPC Shell and Basket Supports at 0.022 seconds for the 100 foot drop of the Transfer Cask onto the Concrete Floor.

Figure A.7 shows the separation between the basket support and MPC shell in the region between the stitch welds. (Note that the actual location of the one inch stitch weld is on the far side of the support since the centerline of the support is on the plane of symmetry.) The figure shows that the shell meridional curvature changes several times in this region. This is due primarily to the constraint of radial displacement caused by the radial contact of the MPC shell with the inner shell of the transfer cask.

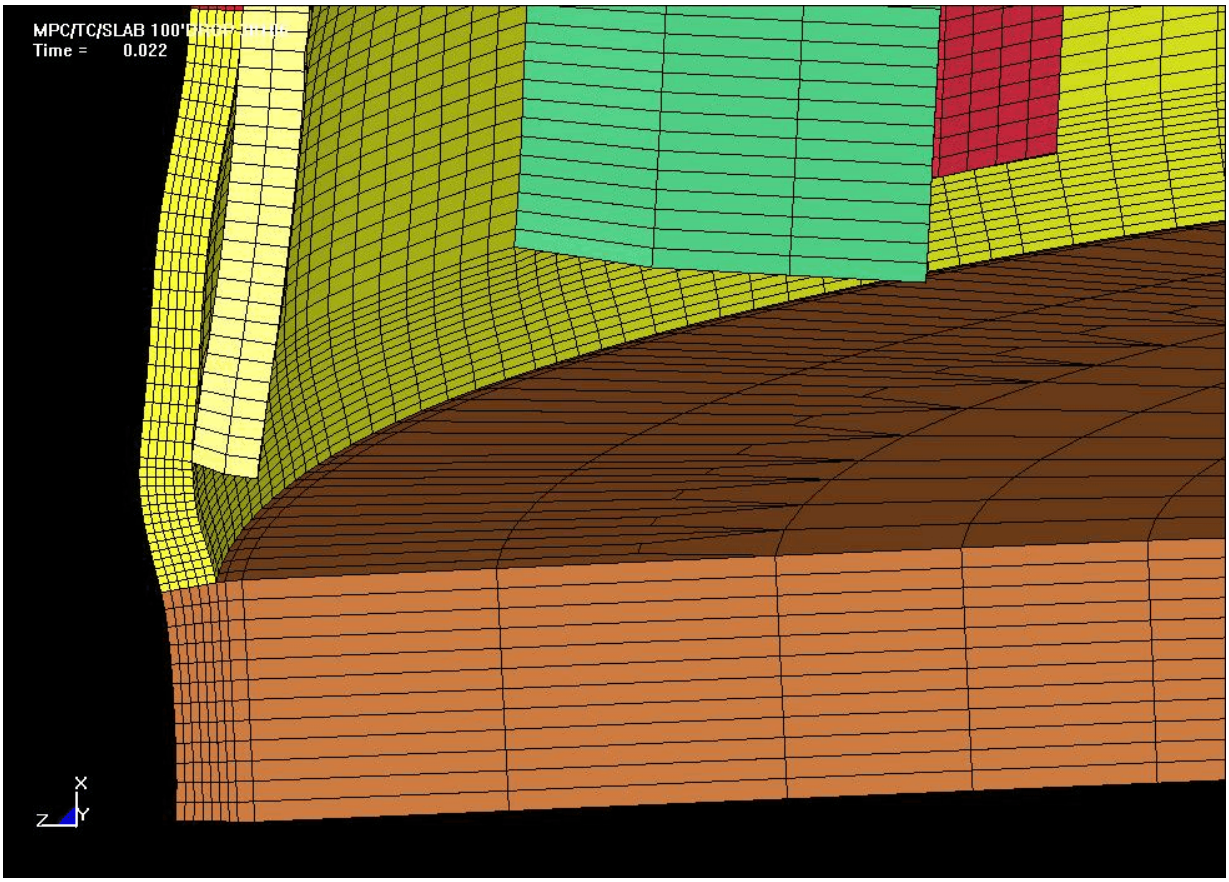

Figure A.7. Deformation of the MPC Shell and Basket Supports at 0.022 seconds for the 100 foot drop of the Transfer Cask onto the Concrete Floor.

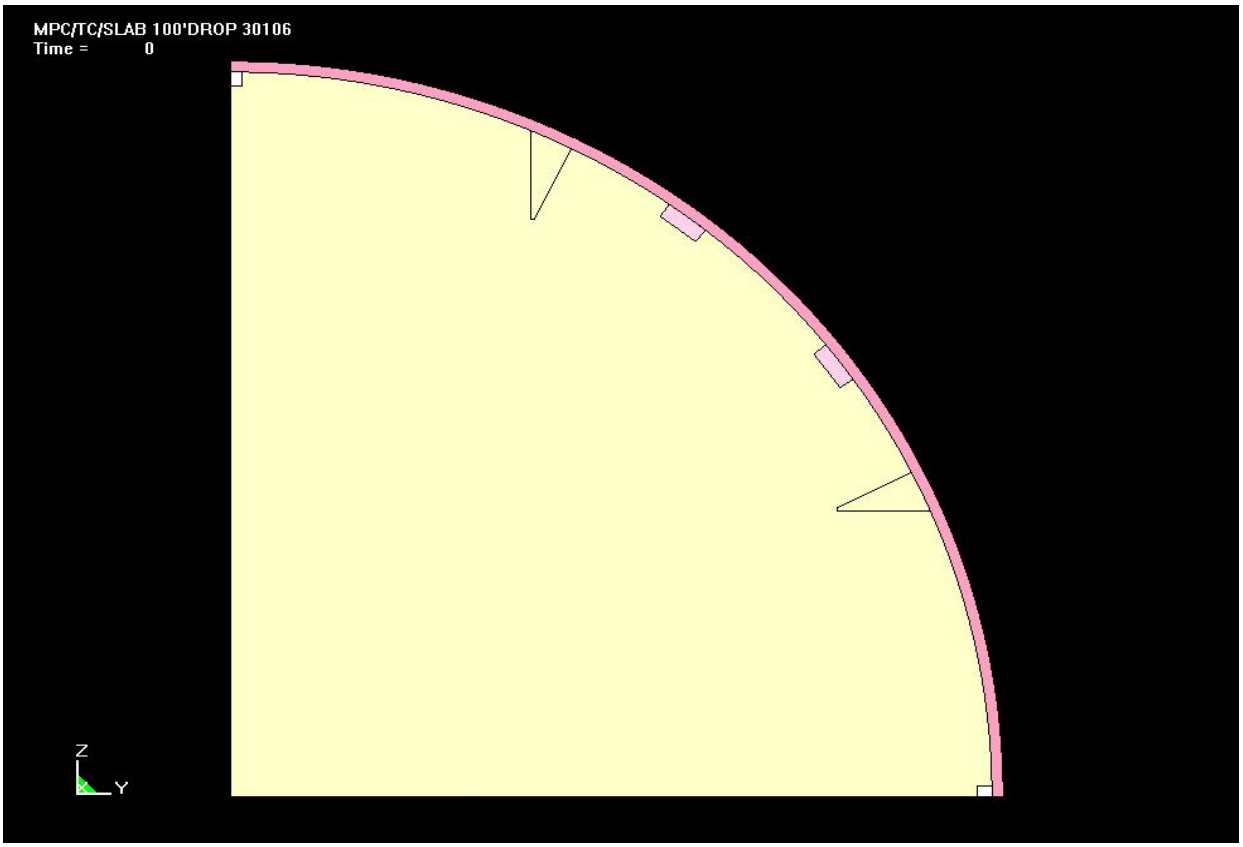

Figure A.8. Plan view of a horizontal section through the MPC shell showing the location of the basket supports.

Figure A.8 is a plan view of a horizontal section through the MPC shell showing the location of the basket supports. Figure A.9 is an elevation view of the MPC shell, baseplate and basket supports in their undeformed position, and Figure A.10 is the same view at the time of maximum response (0.022 seconds). Figure A.11 shows contours of effective plastic strain (EPS) at the time of maximum response, and when viewed together with Figure A.10 shows that the maximum EPS occurs in the shell at the bottom of the supports. Figure A.12 shows the EPS contours along the back of the shell. Both Figures A.11 and A.12 show that the maximum strains occur in the MPC shell region between the bottom of the basket supports and the base plate. Away from the bottom region of the MPC shell, strains diminish rapidly to very small values.

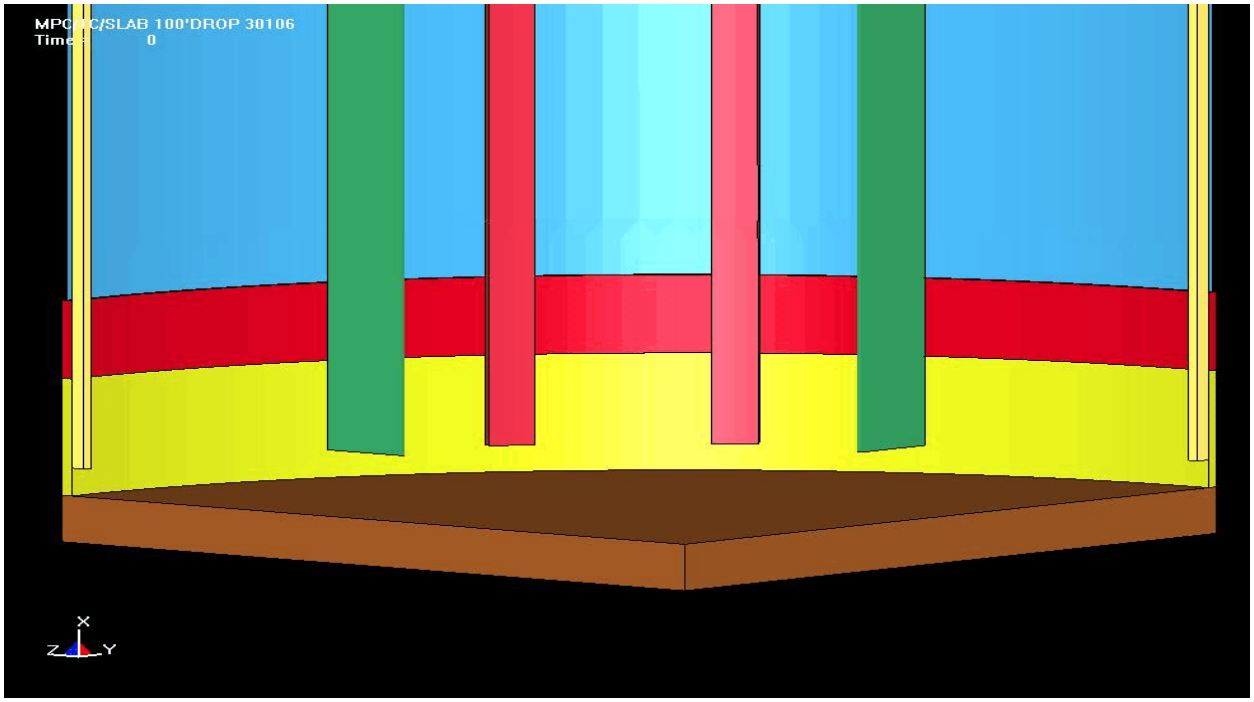

Figure A.9. Elevation view of the MPC shell, baseplate and basket supports in their undeformed position.

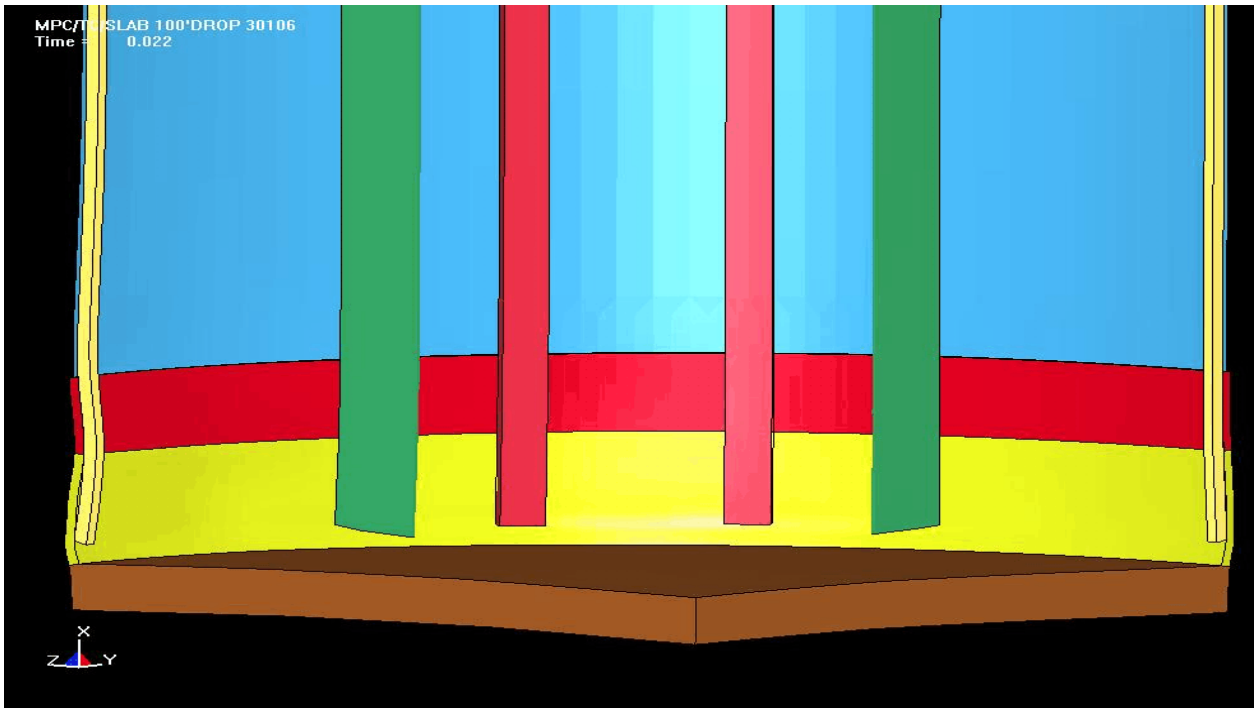

Figure A.10. Elevation view of the MPC shell, baseplate and basket supports at 0.022 seconds. 100 foot drop.

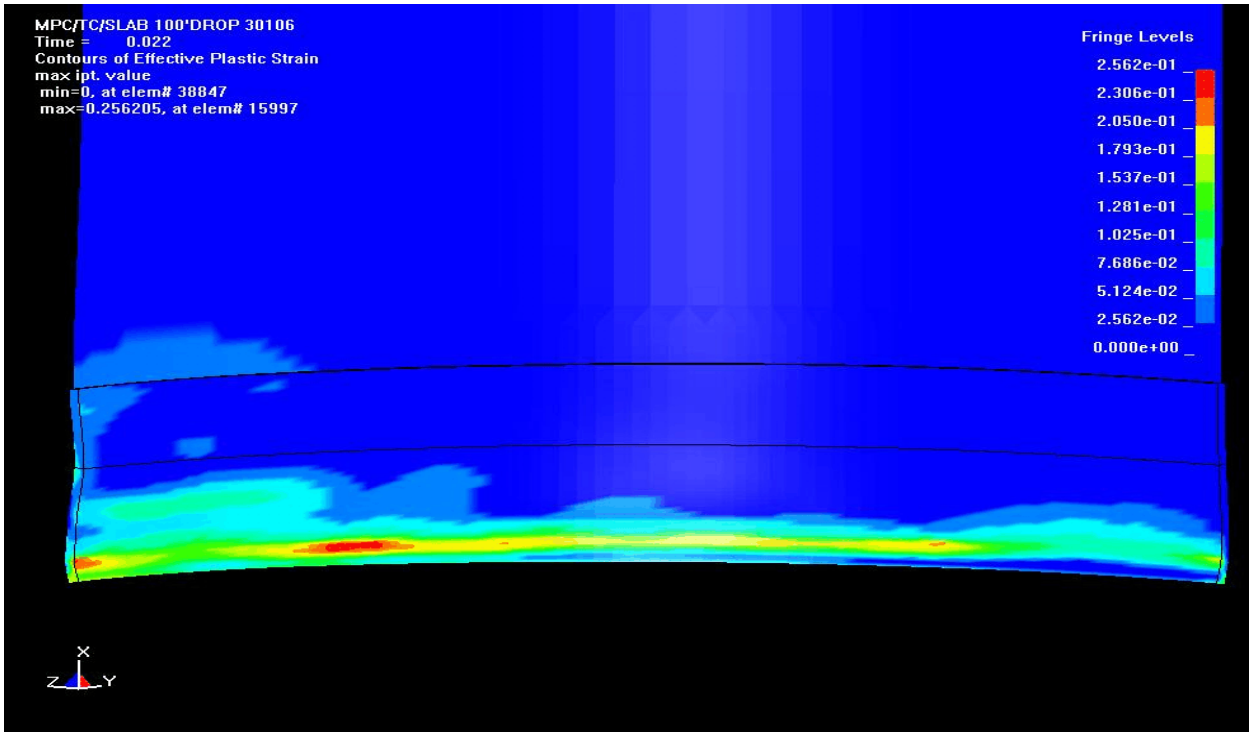

Figure A.11. Contours of effective plastic strain (EPS) on the interior of the MPC shell at the time of maximum response (0.022 seconds). 100 foot Drop.

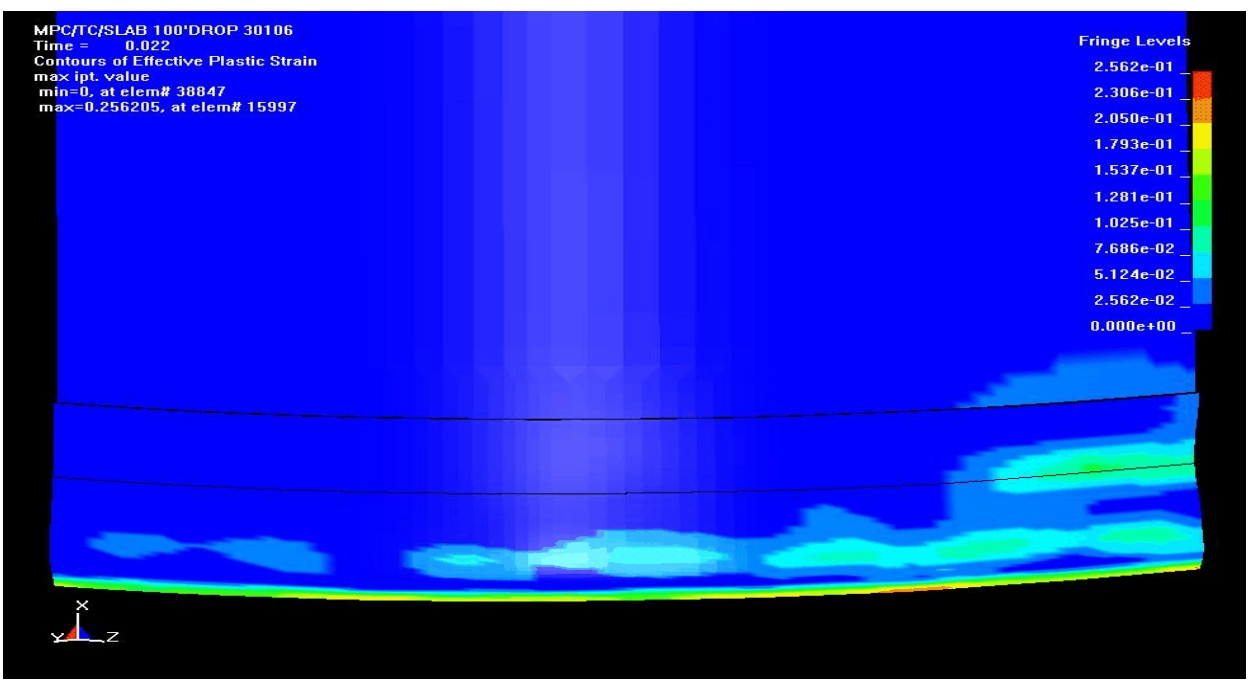

Figure A.12. Contours of effective plastic strain (EPS) on the exterior of the MPC shell at the time of maximum response (0.022 seconds). 100 foot Drop.

Figure A.13 is a close up view of Figure A.11 showing the location of the element with the maximum EPS (Element 15997) and Element 9421 at the junction of the shell and baseplate on the plane of symmetry. Figure A.14 is a vertical section through the MPC shell at the location of Element 15997 and the maximum EPS. Element 15997 is on the inside surface of the shell and Element 15577, also shown in the figure, is on the outside surface at the same elevation. Figure A.15 shows the time history of EPS in each element through the thickness at this location. The figure shows how rapidly the plastic strains diminish from a maximum of 0.256 in/in on the inner surface to a minimum of 0.040 in/in at the outer surface. Figure A.16 shows the time history of EPS in each element through the thickness between Elements 9445 and 9025 at the bottom of the shell where it joins the baseplate. Figure A.16 shows that the EPS in Element 9025, which is at the location of the MPC shell to base plate weld, is 0.220 in/in, which is close to the maximum EPS.

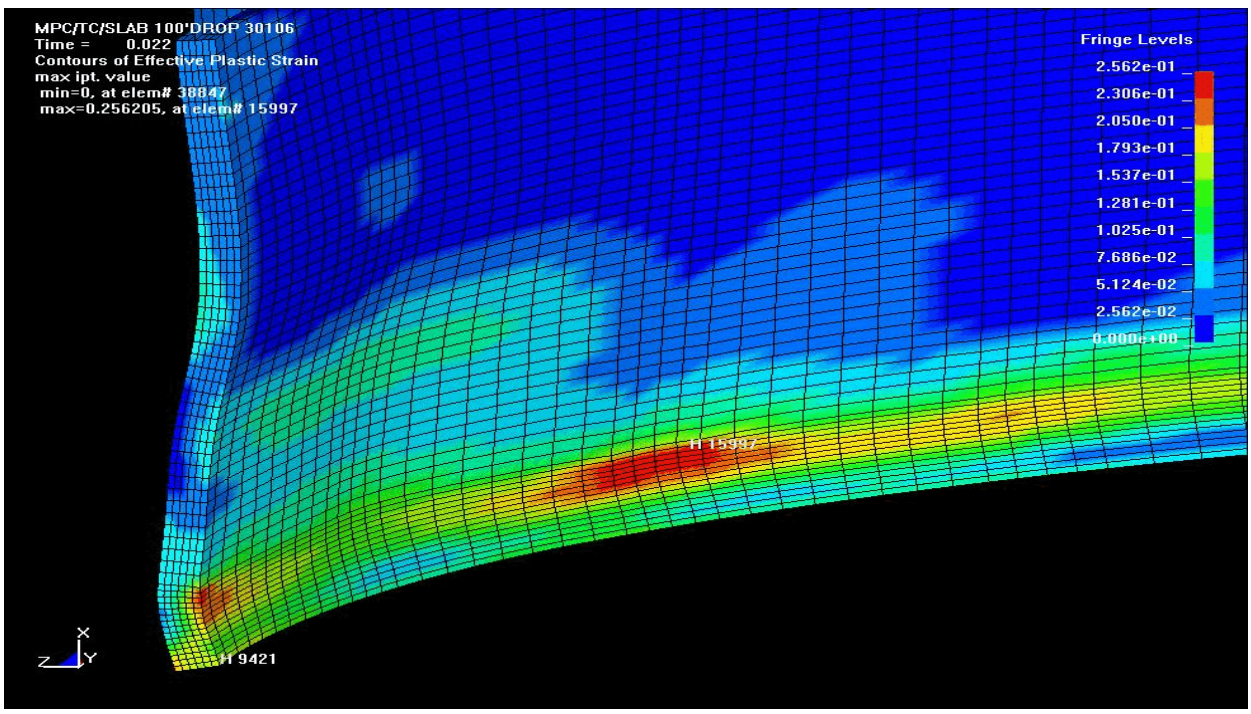

Figure A.13. Close up view of Figure A.11 showing the location of the element with the maximum EPS (Element 15997) and Element 9421 at the junction of the shell and baseplate on the plane of symmetry. 100 foot drop.

In Table A.3, it is tempting to compare the maximum EPS in the element to the true strain at failure. Such a comparison, however, is not an accurate predictor of margin against element failure because these two strain measures, (i.e., calculated maximum EPS and true strain at failure), are each derived from different states of stress and must be adjusted by a Triaxiality Factor before a meaningful comparison can be made. The derivation of the Triaxiality Factor and its application to predicting material failure in the MPC is discussed in Appendix B.

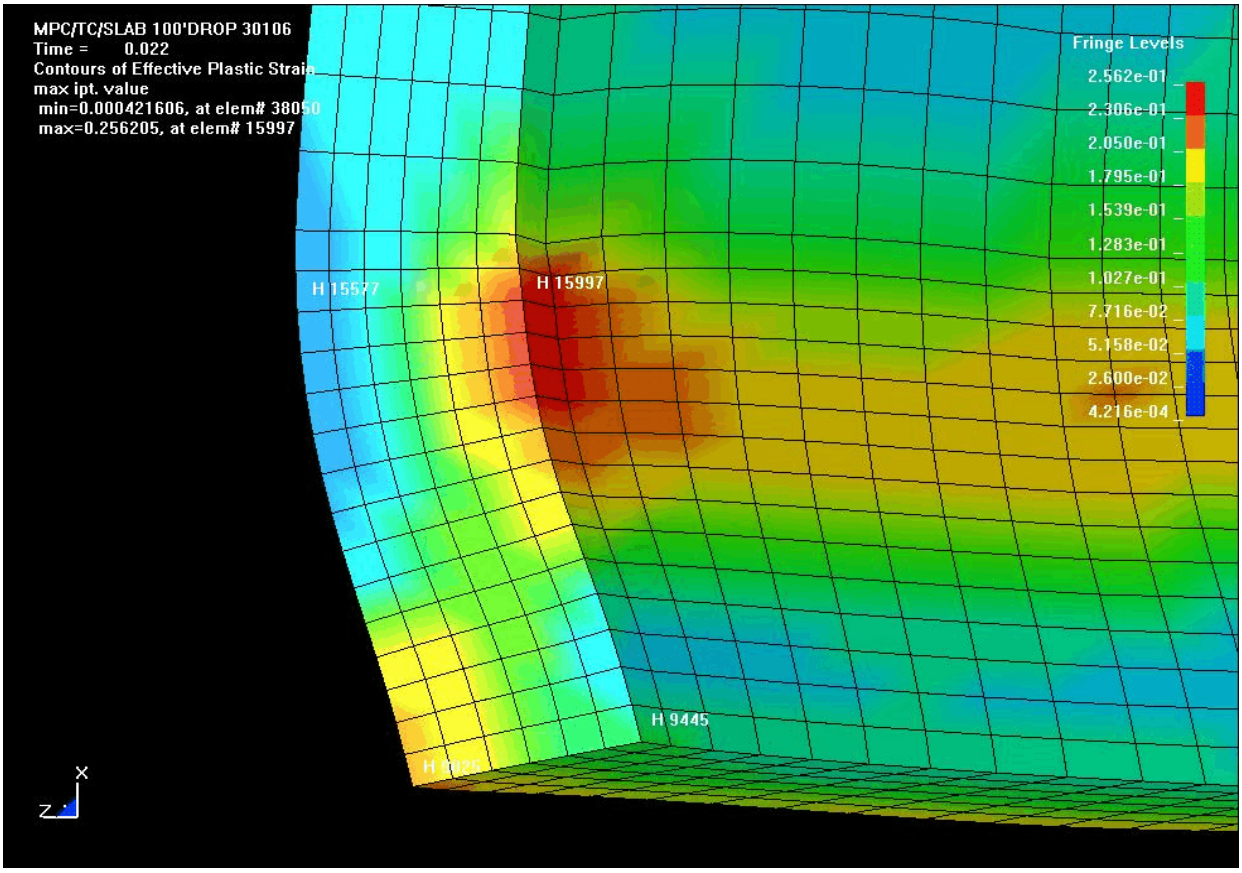

Figure A.14. Vertical section through the MPC shell at the location of Element 15997 and the maximum EPS. 100 foot drop.

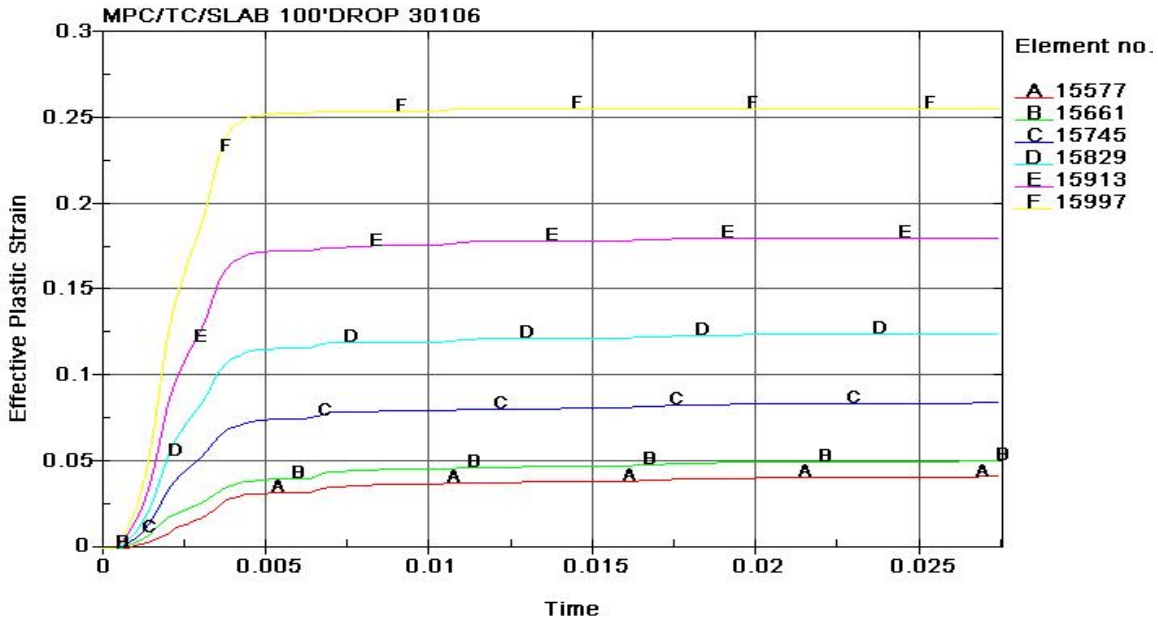

Figure A.15. Time history of EPS in each element through the thickness at the location of the maximum EPS. 100 foot drop.

A.4.4. Question 4

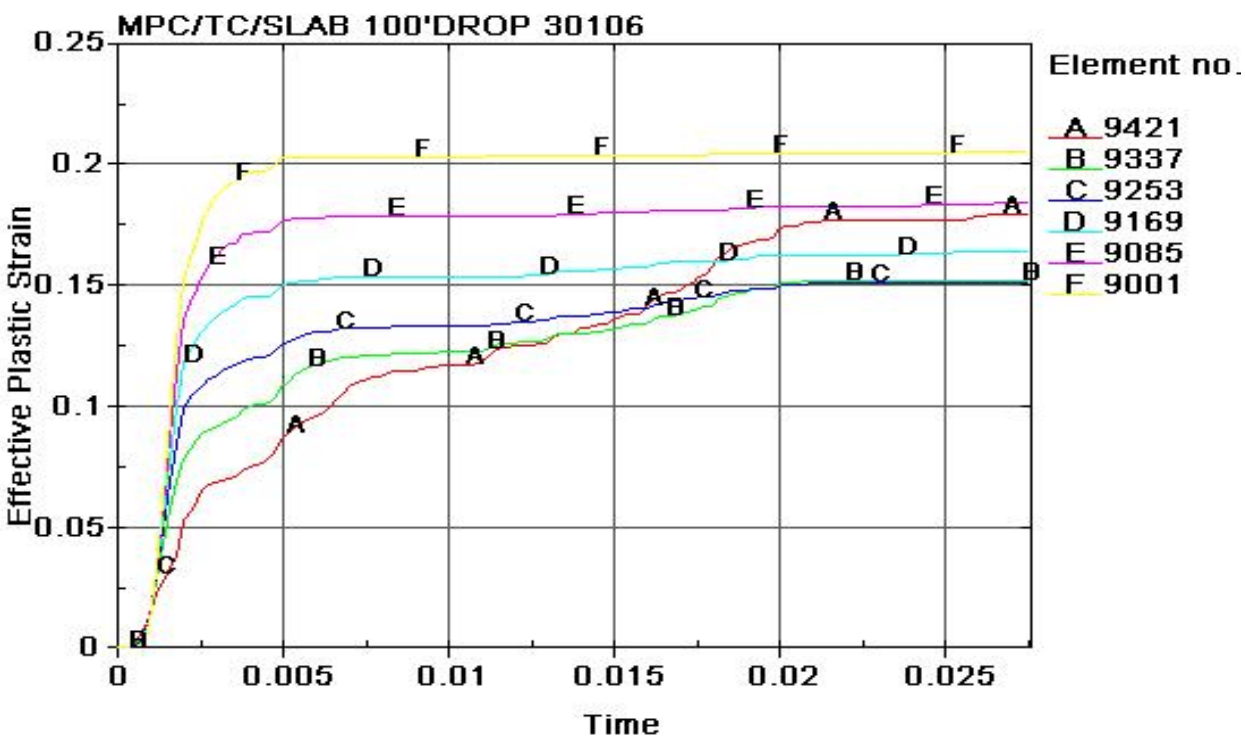

Figure A.16. Time history of EPS in each element through the shell thickness at the location of the MPC base plate on the plane of symmetry. 100 foot drop.

Analyze the vertical drop of the transfer cask containing a sealed MPC falling onto the storage overpack at ground elevation from heights of 1.5, 12.2, and 24.4 m (5, 40, and 80 ft). Determine the magnitude and location of maximum stresses/strains in the MPC.

To respond to this question, dynamic analyses using LS-DYNA were performed for the accidental vertical drop of the transfer cask onto the storage overpack, while the transfer cask is being lowered from the operating floor to the ground floor. The maximum drop height corresponds to the distance between the operating floor and the top of the storage overpack, which could be up to 24.4 meters (80 feet). Several drop heights up to the maximum height were analyzed.

The finite element model of the transfer cask (transfer overpack, MPC, and internals), utilized for this drop case, is the same model used in the response to Question 3 except for the MPC, which did not include the modifications stated above. A finite element model of the storage overpack was also developed and placed beneath the transfer cask model. A quarter model representation of the storage overpack was created to be consistent with the quarter model transfer cask. The storage overpack model consists of a 68 cm (26.8 inches) thick concrete cylinder with steel plates on the top, inside, and outside surfaces of the concrete wall. The concrete and steel plates are modeled using brick type finite elements. The material model and properties for the concrete cylinder are the same as those described in the response to Question 3. The material model and properties for the steel plates are taken at room temperature. The bottom of the storage overpack is restrained in the model. This is slightly conservative, since it is actually resting on the concrete floor that is supported by a concrete wall beneath the floor.

The drop heights selected for analysis were 1.52, 12.2, and 24.4 m (5, 40, and 80 ft). The MPC stainless steel material properties correspond to a temperature of 237°C (459°F), which is the temperature used by the manufacturer for the design of the MPC. The structural response of the MPC is presented in Table A.4.

Table A.4. Structural Response of MPC

Drop Height m (ft)	[1]Max. EPS at Element 9421 (Azimuth = 0) cm/cm (in/in)
1.52 (5)	0.0363 [2]
12.2 (40)	0.0601 [2]
24.4 (80)	0.0976 [2]

[1] EPS is the effective plastic strain; element no. 9421 is the first MPC vertical brick element at the plane of symmetry.

[2] The drop of the transfer cask onto the storage overpack is a softer impact than the drop of the transfer cask onto the concrete floor. Therefore, the resulting strain in the MPC is less at the higher (40 ft and 80 ft) drop heights. The result for the 5 ft drop is larger than the result for the 5 ft drop onto the concrete floor because (a) the difference in target stiffness has less effect at lower drop heights, and (b) the modifications to the model discussed in response to Question 3 were not made to this model because it produced very conservative results that were bounded by the 40 ft, 70 ft, and 100 ft drops onto the concrete floor.

A.4.5. Question 5

Determine the magnitude and location of maximum stresses/strains in the MPC when a sealed MPC vertically falls 5.8 m (19 ft) into the storage overpack.

Such an event could occur during the transfer of the MPC from the transfer overpack to the storage overpack.

When the MPC is moved from the transfer overpack to the storage overpack (Stage 21), it could possibly fall a maximum of 5.8 m (19 ft). This load drop is analyzed using a finite element model.

Model Development

The finite element model includes the MPC, storage overpack inner shell, storage overpack vertical channel sections, and the storage overpack bottom lid (which serves as the target plate). The analysis strategy and the finite element models of the MPC, fuel assemblies, fuel basket and fuel basket support are the same as those used in response to Question 3. These components are shown in Figures A.17 and A.18. The finite element model (FEM) shown in Figure A.17 is a quarter-model representation of the cask system (due to symmetry about two vertical planes). Figure A.18 shows a close-up view at the MPC connection to the MPC bottom baseplate at the plane of symmetry. The fuel basket plate on the plane of symmetry has been removed, so that the fuel assemblies within the basket compartments can be seen.

The top plate of the storage overpack bottom lid is modeled as a rigid target plate for the vertical impact

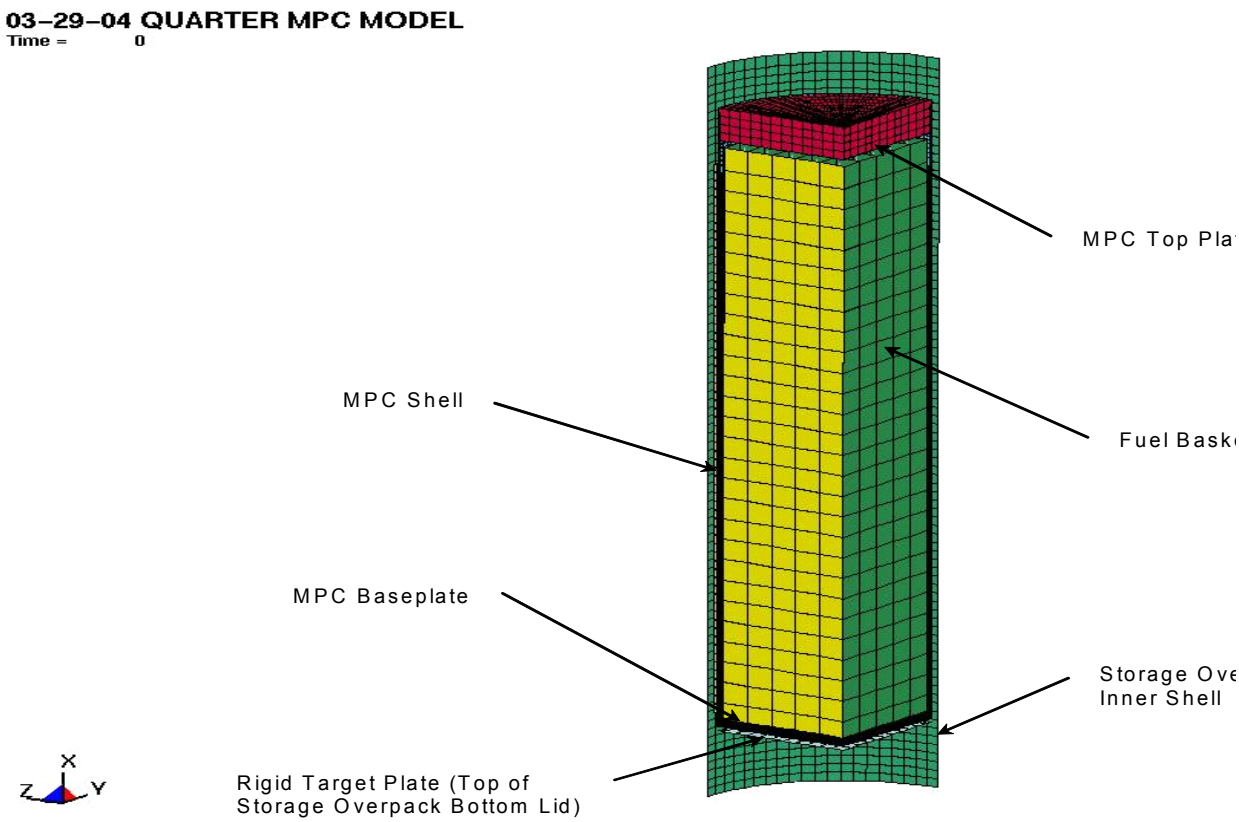

Figure A.17. Finite Element Model of the MPC for 19 Ft Drop into Storage Overpack

of the MPC and its internal components. The target plate is fully restrained in the model because:

- The storage overpack bottom lid is considered to be rigid since it is constructed from a 12.7 cm (5 inch) top plate, a 5.1 cm (2 inch) bottom plate, and 43.2 cm (17 inches) of confined concrete between the plates, and

- The storage overpack rests on a reinforced concrete floor supported by a reinforced concrete wall beneath the floor. The assumption of a rigid target plate for this drop scenario is conservative.

The storage overpack vertical wall is modeled using a rigid shell to represent the storage overpack inner steel shell, which surrounds the MPC shell wall. The vertical channels, which are welded to the storage overpack inner shell, are included in the model using shell elements. The gap between the channel webs and the MPC shell wall is included in developing the model.

For this drop scenario, a dynamic analysis was performed using LS-DYNA. The MPC and internal components rest on the target plate at the start of the analysis, and the drop height was simulated by introducing an initial velocity that was calculated using the expression:

$$V = \sqrt{2gh} \qquad (A.7)$$

where: V = velocity
g = gravitational acceleration
h = drop height.

To permit the insertion of the MPC into the storage overpack, the cask design specified a gap between the MPC shell wall and the inner radius of the vertical channel sections welded to the storage overpack inner shell. If the MPC impacts the bottom lid of the storage overpack in the center, there would be a uniform gap equal to 1.67 cm (0.657 inches) based on average construction tolerances or a uniform gap of 2.18 cm (0.859 inches) based on maximum construction tolerances. Under this configuration, when the MPC shell deforms radially by an amount greater than the uniform radial gap, the channel sections attached to the storage overpack provide resistance to further radial deformation. For the analysis reported herein, a worst case assumption was made that during the accidental drop of the MPC, it may land completely to one side of the storage overpack bottom lid. This creates a maximum gap on the opposite side equal to approximately 3.34 cm (1.313 inches) based on average construction tolerances. This off-center drop location is simulated in the analysis by removing from the computer model the contact definition between the MPC shell and the storage overpack channel sections. This permits the MPC shell to deform radially outward without the resistance provided by the channel sections. In this way the analysis can provide an estimate of the effect of an off-center drop.

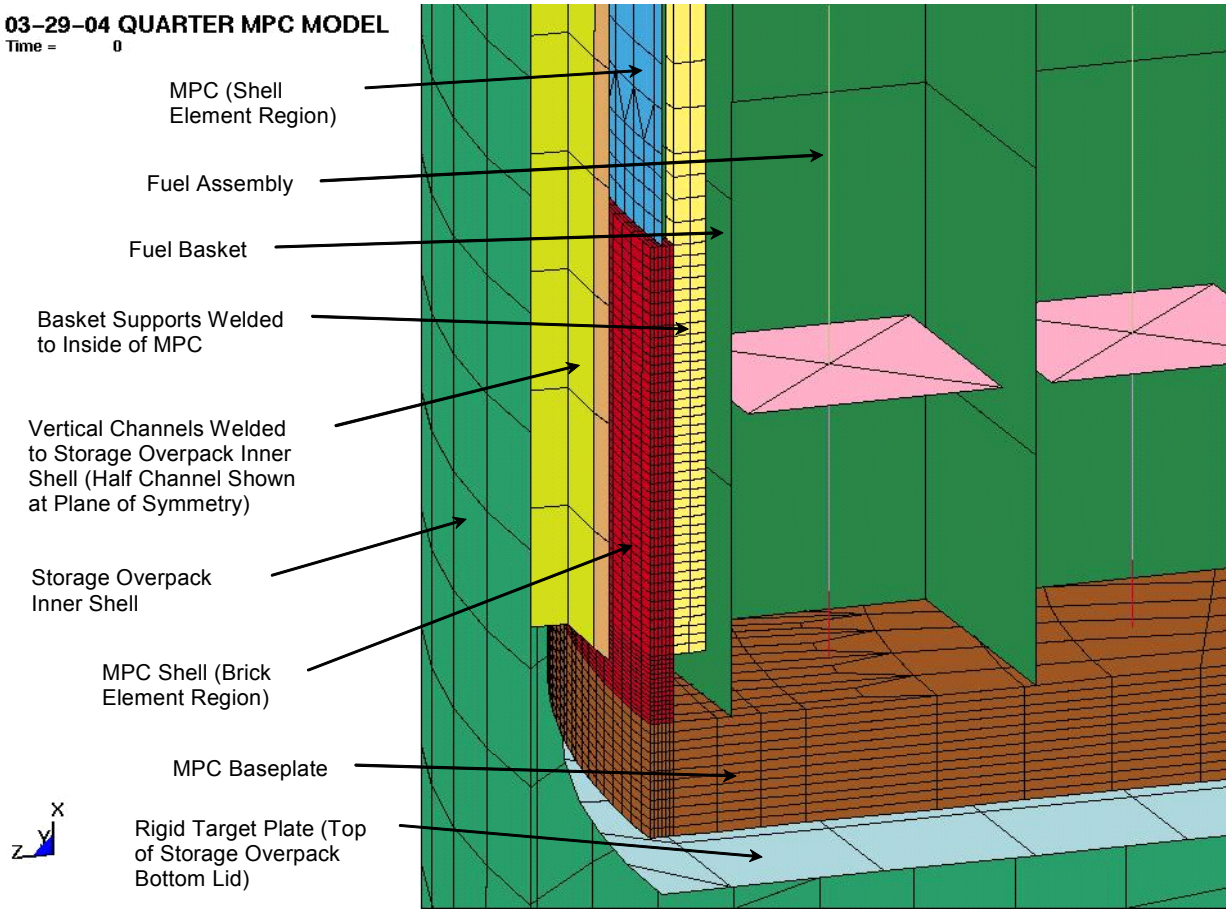

Figure A.18. MPC 19 Ft Drop into Storage Overpack. View of Model at MPC Shell Wall Connection to Baseplate at Plane of Symmetry

Analysis Results

Figure A.19 shows the displacement of the MPC shell and basket support on the xz plane of symmetry at the time of maximum displacement (0.005 seconds) . Figures A.20 and A.21 are plots of radial (z) and vertical (x) displacements at the three nodes located on the MPC shell in Figure A.19. The maximum radial displacement is less than the maximum gap of 1.313", and therefore no contact occurs between the MPC shell and the channel sections attached to the inside of the storage overpack. The curvature of the shell and basket support, as well as the contact and separation between the shell and support can be clearly seen. In contrast to Figure A.7, where the radial displacement was limited by contact with the transfer overpack, Figure A.19 shows a smoother variation in curvature due to the fact that radial displacement is allowed to occur freely.

Figure A.22 shows the contours of effective plastic strain (EPS) in the MPC shell, basket supports and base plate at the time of maximum response, which is the time in Figure A.23 when the kinetic energy of the system is a minimum. Figure A.22 shows that the EPS is 0.459 in/in and occurs in Element 9035. With the basket supports removed, Figures A.24 and A.25 show the location of Element 9035 where the maximum EPS occurs. This element is located at the bottom of the shell on the outside surface within the weld joining the shell to the base plate. Figure A.26 is the same view as Figure A.25 except the basket support is included and the element mesh is defined.

Figure A.27 is a vertical section through the shell and baseplate at the location of Element 9035. The figure shows the relative displacement between the shell and basket support. Because the stiffness of the basket support at this location is so much greater than the basket support on the plane of symmetry (Figure A.19) the shell does not separate as much from the basket support between the stitch welds. Figure A.28 is the displacement history of node 20340 shown in Figure A.27, and shows that the maximum radial displacement is about the same as it is on the plane of symmetry.

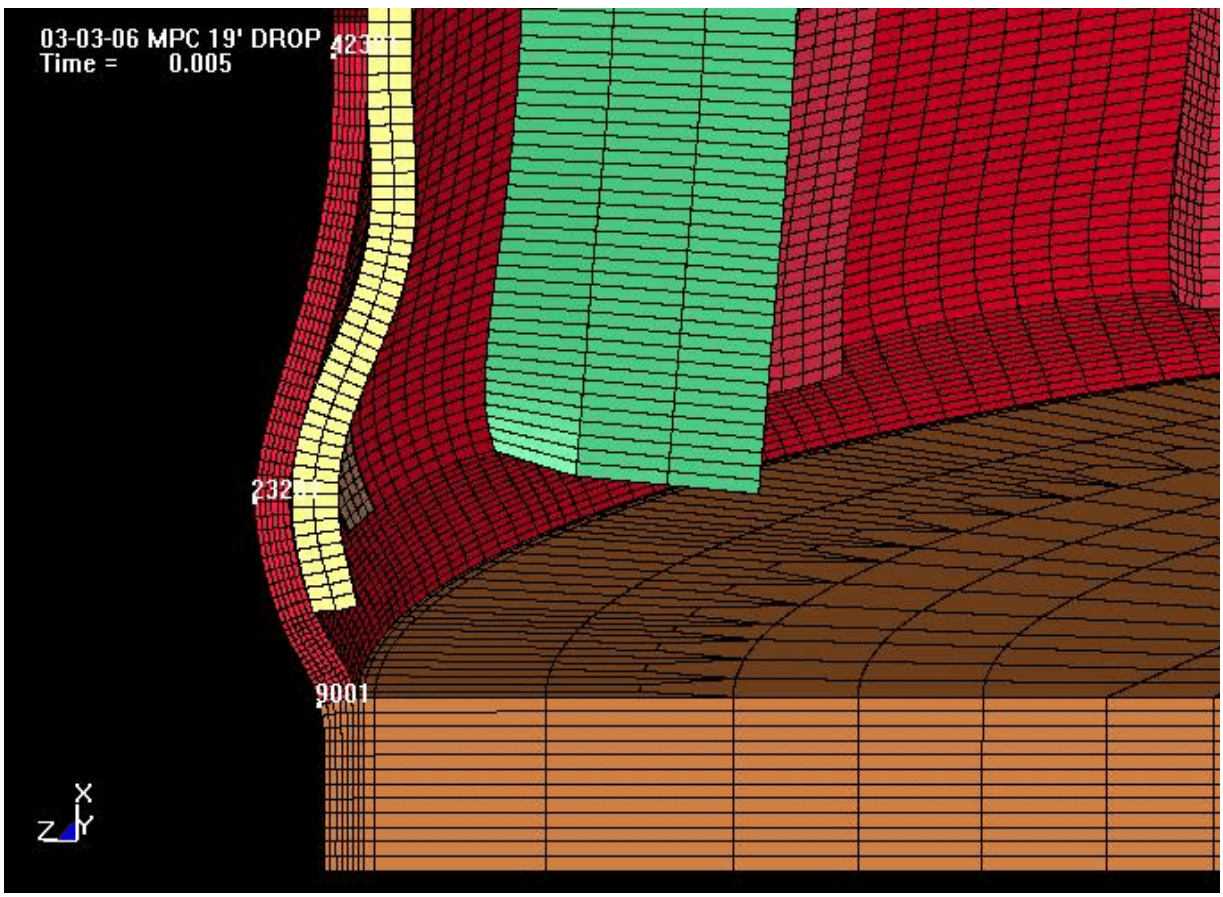

Figure A.19. Displacement of the MPC shell and basket support along the xz plane of symmetry at the time of maximum displacement (0.005 seconds) .

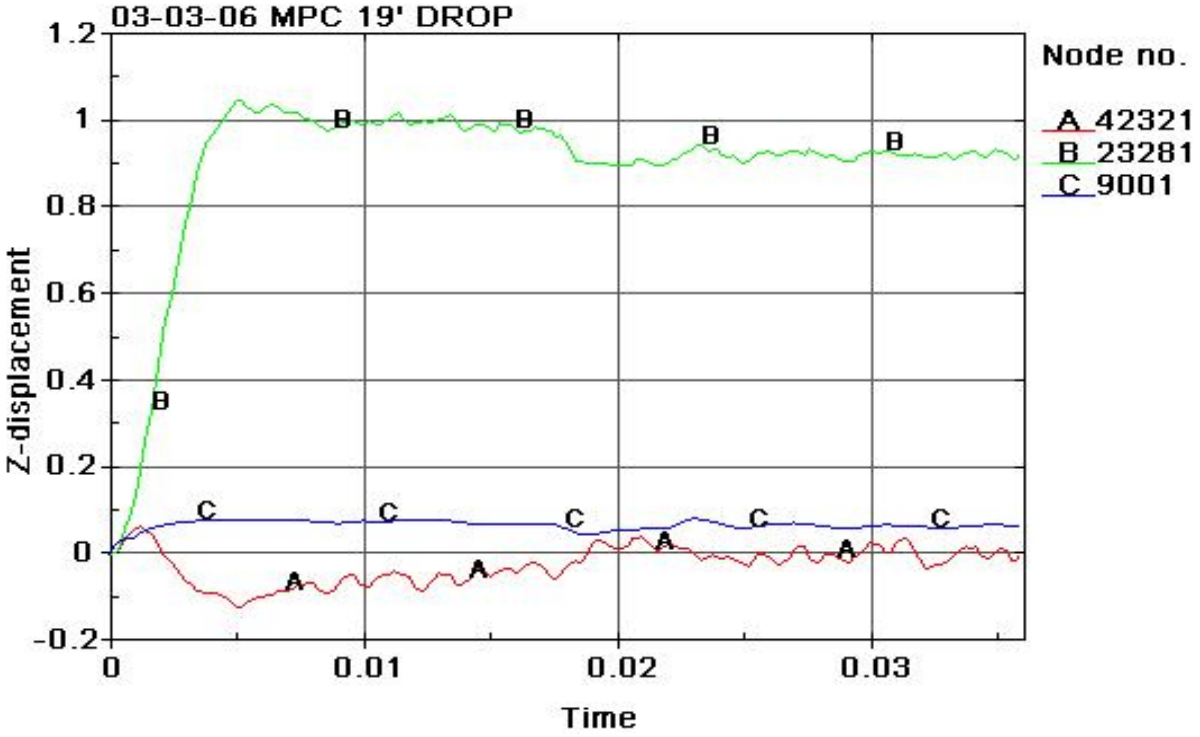

Figures A.20. Plots of radial (z) displacement at the three nodes located on the MPC shell in Figure A.19.

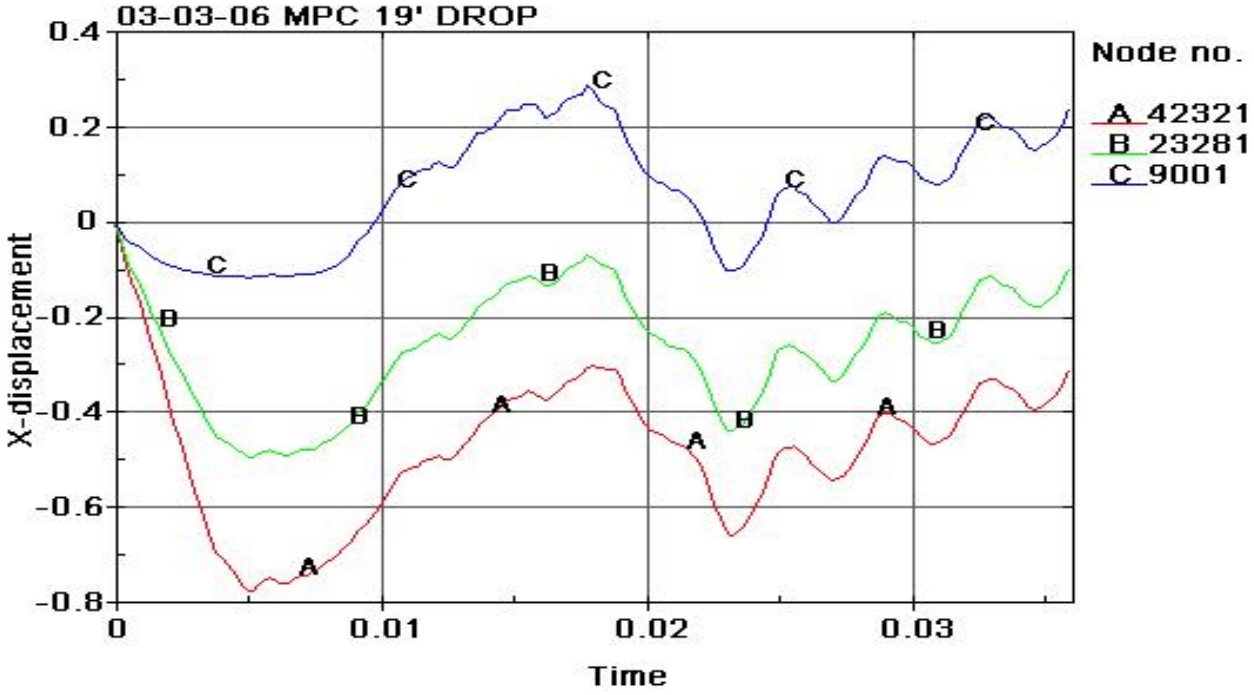

Figures A.21. Plots of vertical (x) displacement at the three nodes located on the MPC shell in Figure A.19.

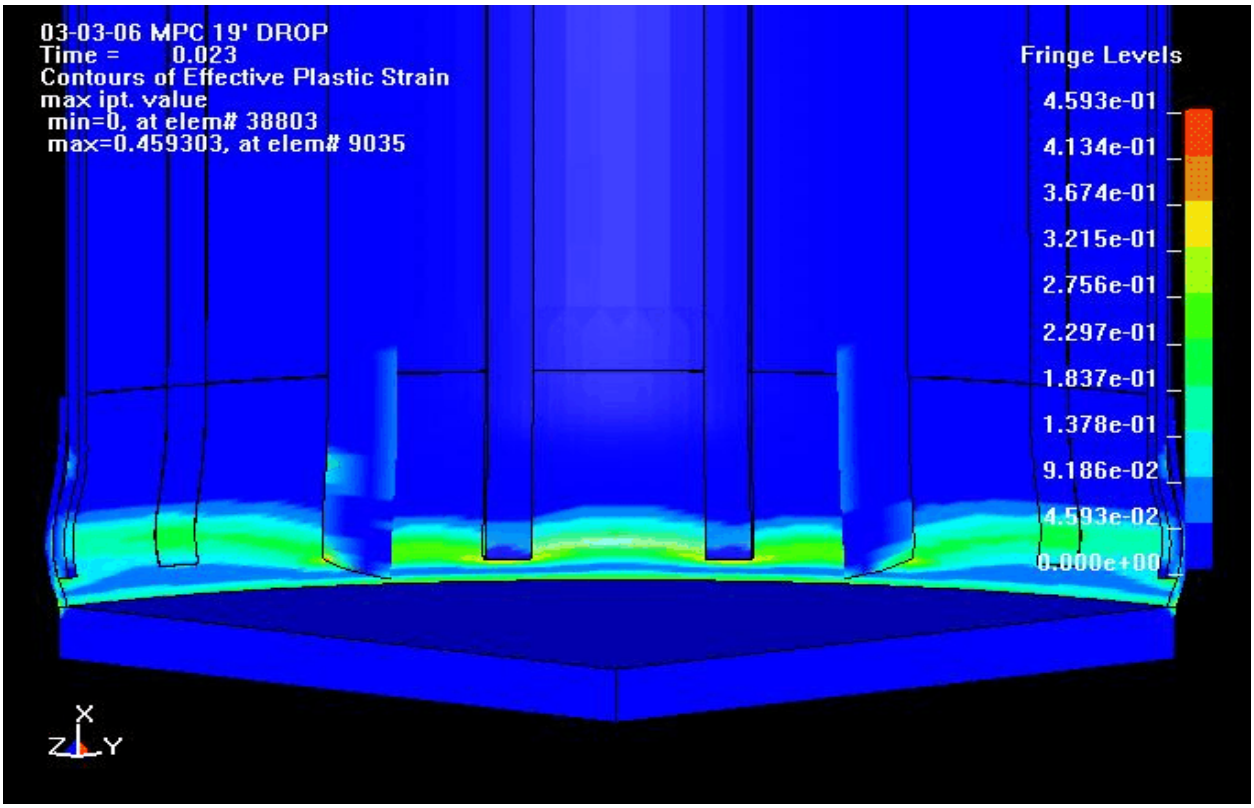

Figure A.22. Contours of effective plastic strain (EPS) in the MPC shell, basket supports and base plate at the time of maximum response, which is the time in Figure A.23 when the kinetic energy is a minimum.

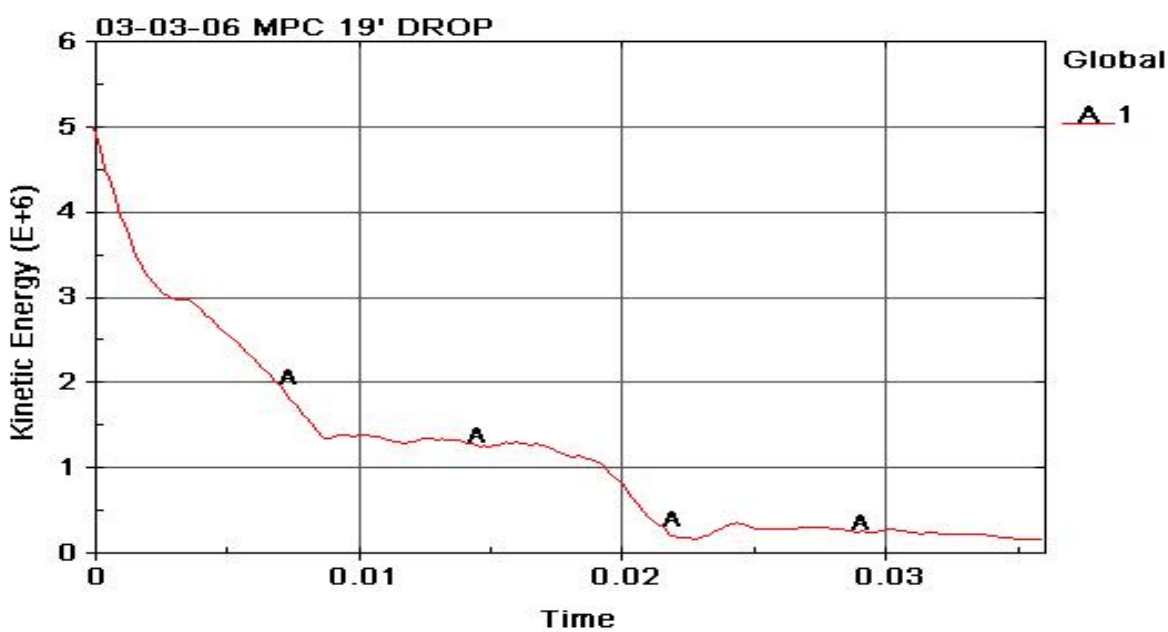

Figure A.23. Global System Kinetic Energy.

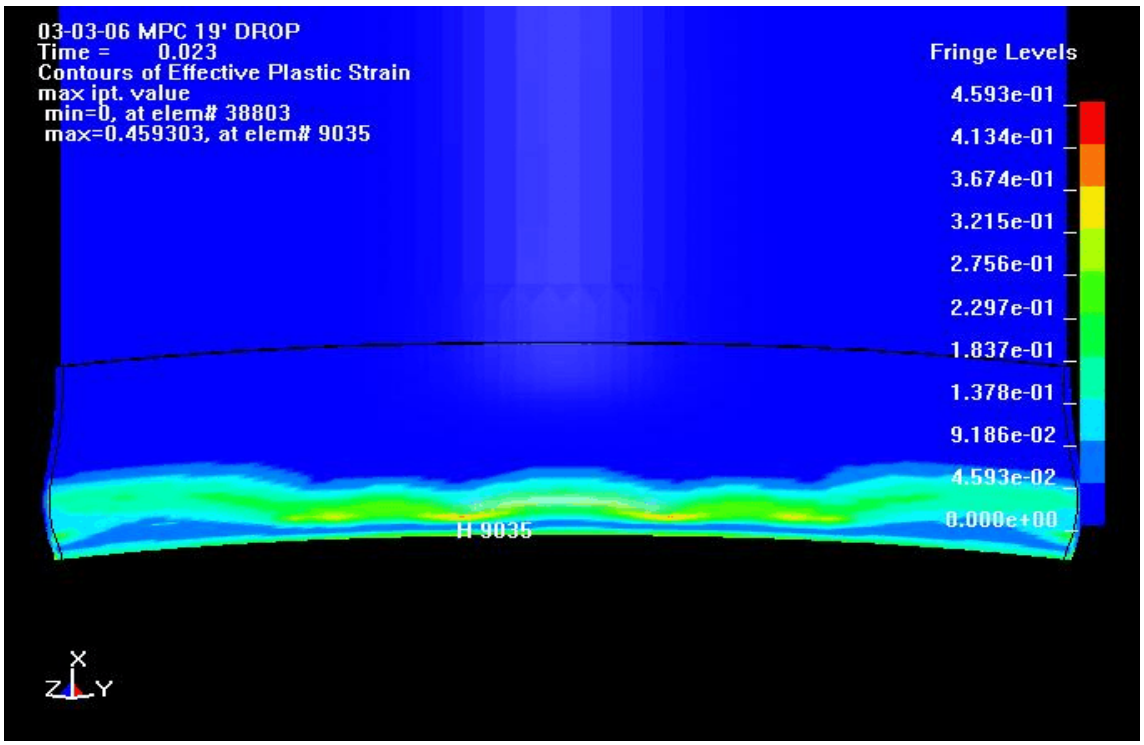

Figure A.24. With the basket supports removed from Figure A22, Figure A.24 shows the location of Element 9035 where the maximum EPS of 0.459 occurs.

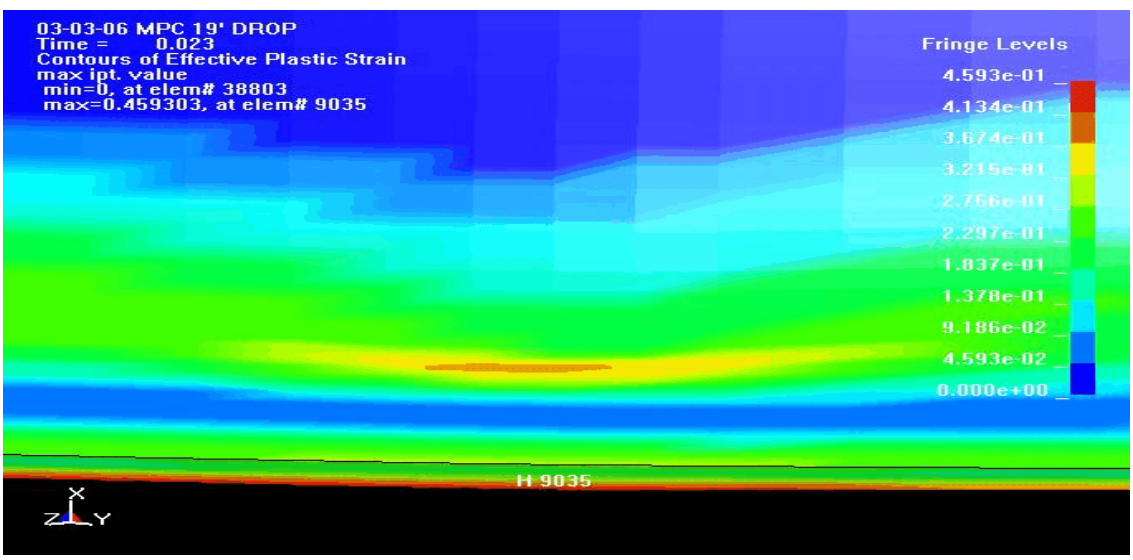

Figure A.25. Closeup view of the location of Element 9035 on the bottom outside edge of the MPC shell.

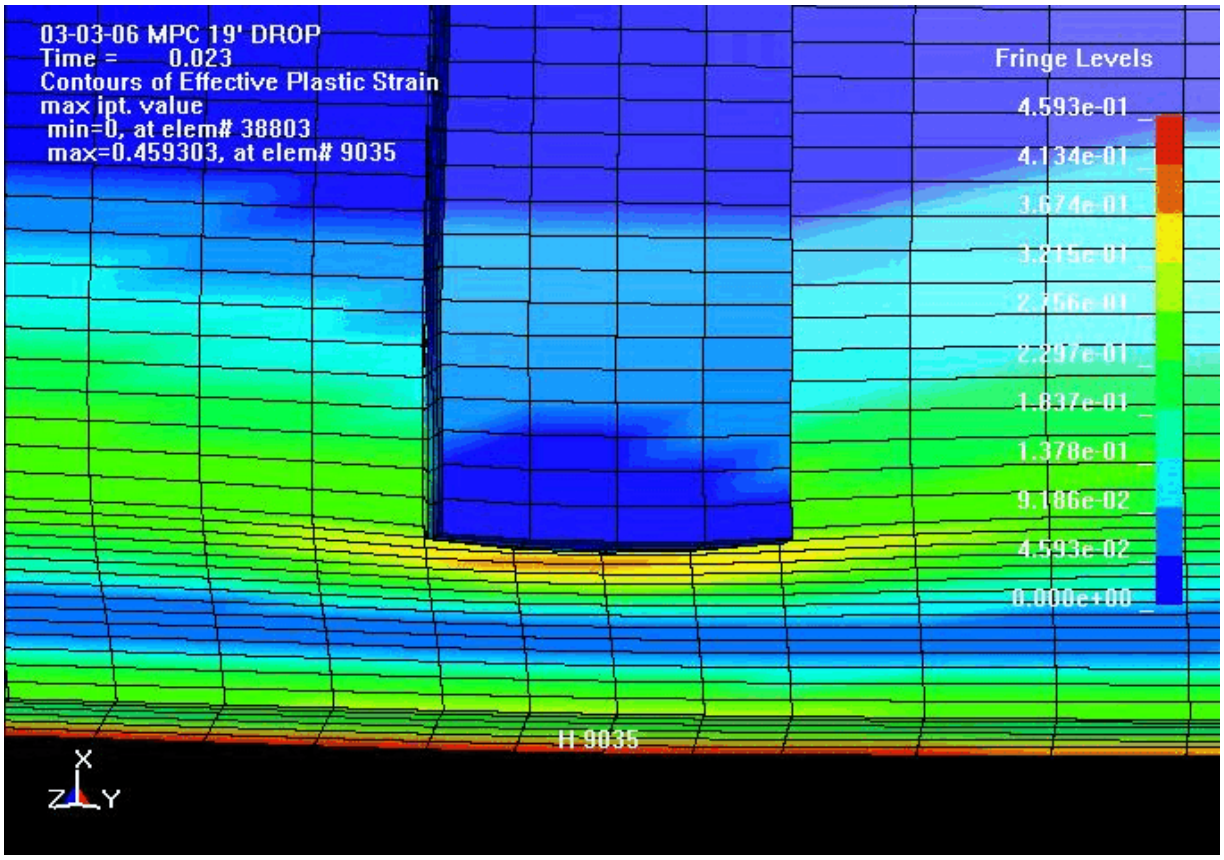

Figure A.26. Same view as Figure A.25 except the basket support is included and the element mesh is defined.

Figure A.29 is a vertical slice through the MPC shell and base plate showing the location of Element 9035 and the local distribution of EPS within the shell. Figure A.30 labels the elements through the shell thickness at the junction of the shell and base plate, and Figure A.31 plots the time history of EPS within each element. These plots show the significant decrease in the maximum EPS away from the outside surface of the shell.

The 19 foot drop of the MPC into the storage overpack produces the highest EPS (0.459 in/in) of any of the cask and MPC drop events. This event, and the probability of breaching the MPC confinement boundary are discussed in greater detail in Appendix B.

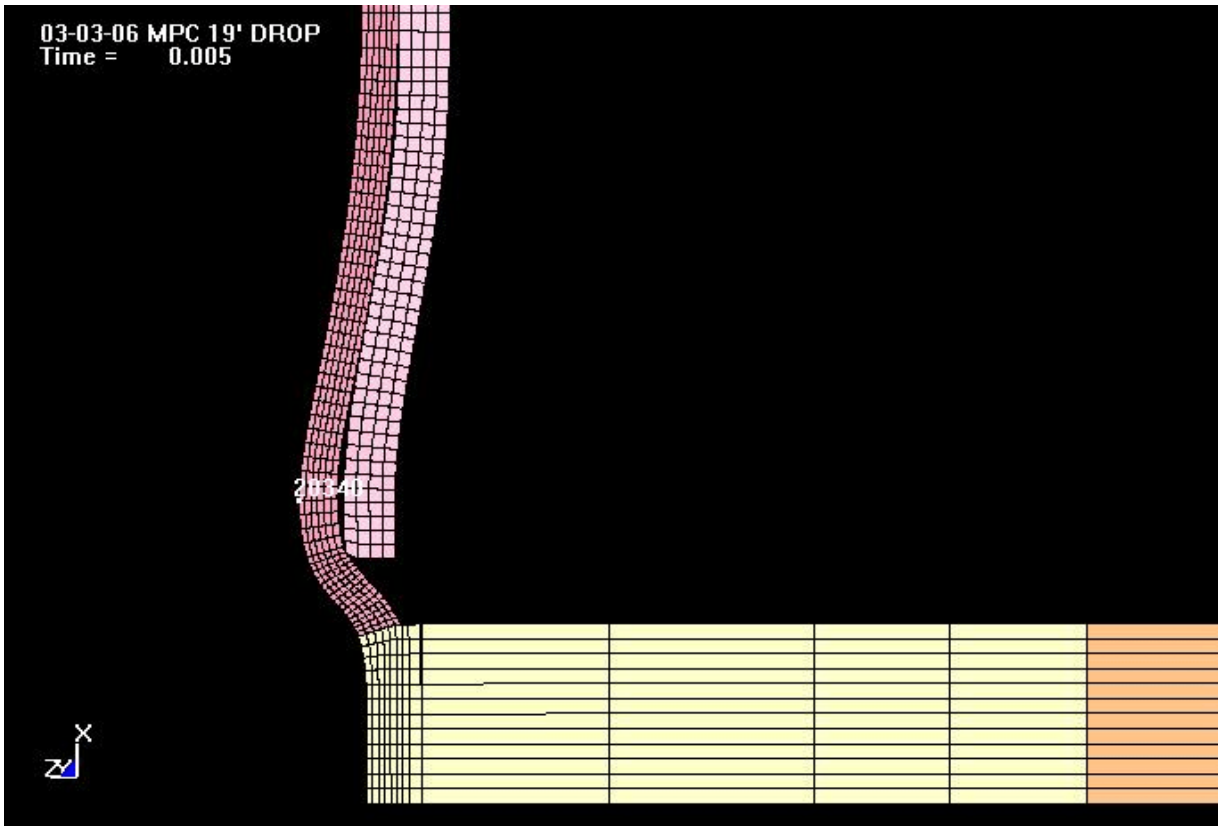

Figure A.27. Vertical section through the shell and baseplate at the location of Element 9035 showing the relative displacement between the shell and basket support.

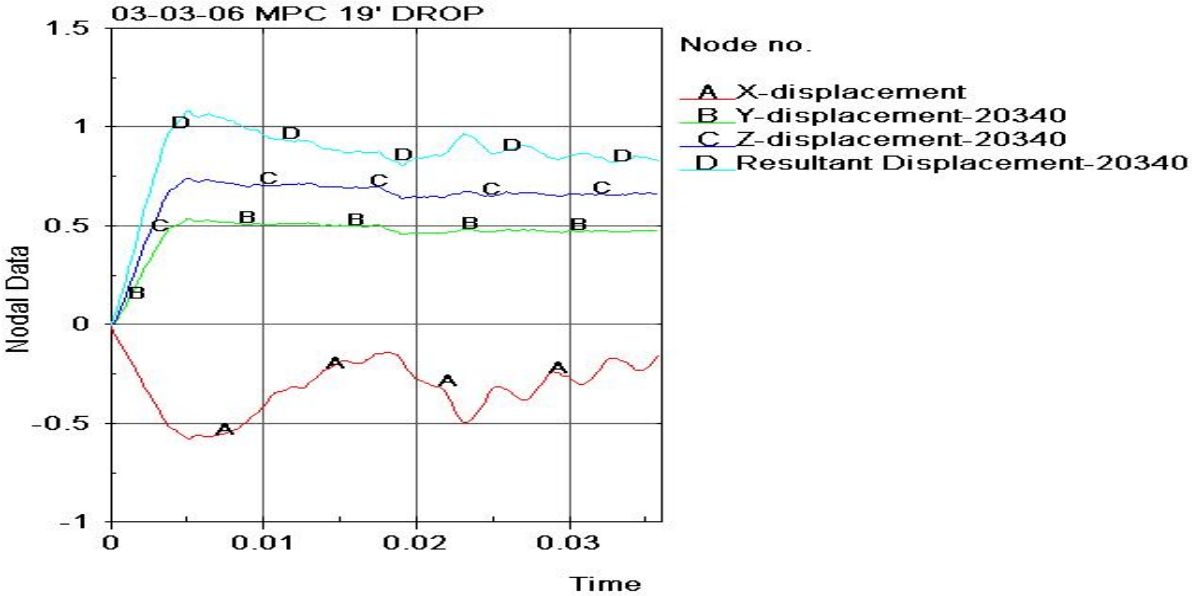

Figure A.28. Displacement history of node 20340 shown in Figure A.27.

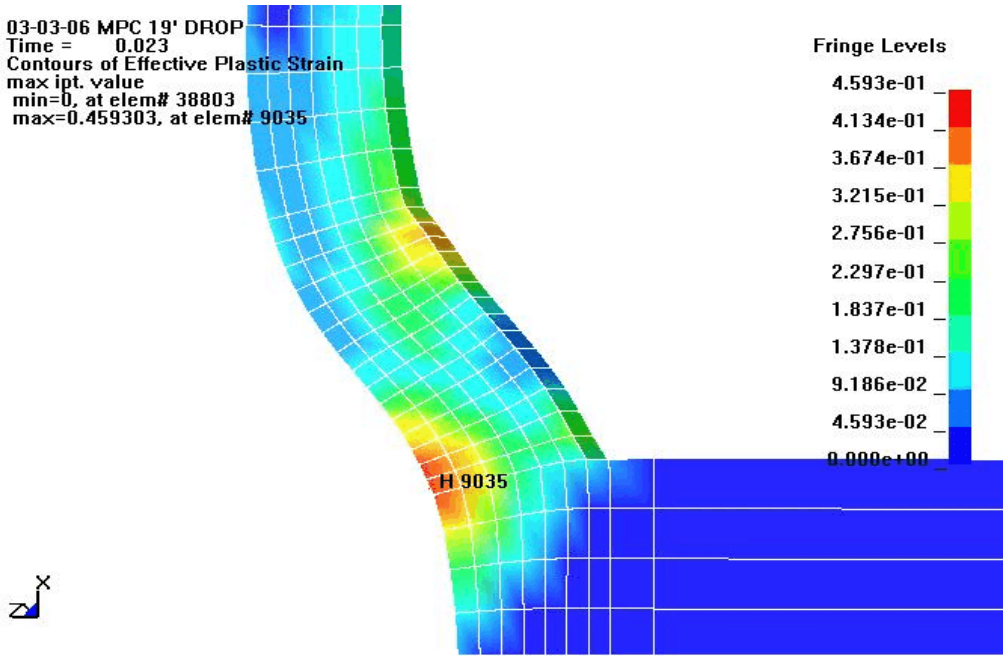

Figure A.29. Slice through the MPC shell and base plate showing the location of Element 9035 and the local distribution of EPS within the shell.

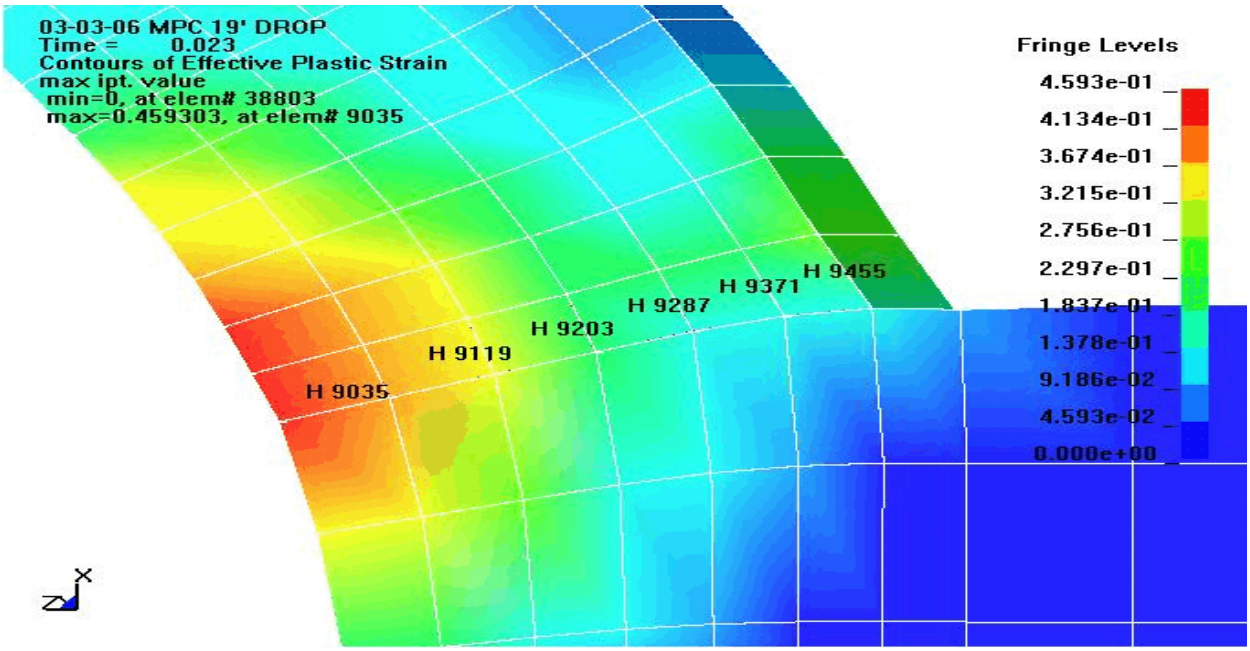

Figure A.30. Labels the elements through the shell thickness at the junction of the shell and base plate at the location of maximum EPS.

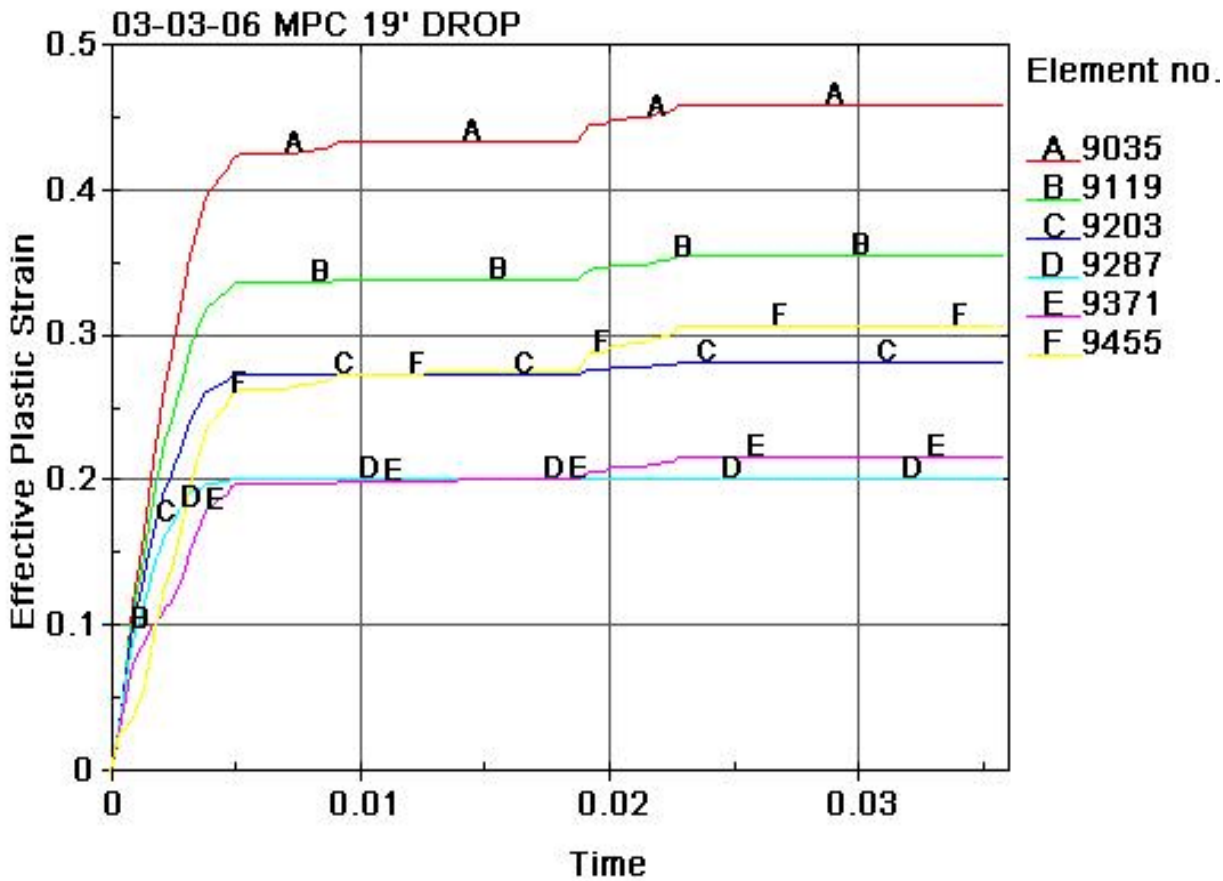

Figure A.31. Time history of EPS within each element through the thickness as shown in Figure A.30.

A.4.6 Question 6

If the storage cask drops onto the Independent Spent Fuel Storage Installation (ISFSI) concrete pad, asphalt area, or gravel area, will it slide and/or tip-over? If tip-over can occur, what velocity of the crawler would be required to tip it over? How much time does the operator have to stop the crawler before tip-over occurs? What are the stresses in the MPC?

The storage cask is hung from the top while being transported by the crawler. To perform this calculation a few assumptions were made based on photos and a drawing of the crawler. The height of the storage cask above the ground surface before the drop occurs is assumed to be 30.5 cm (12 inches). The crawler is traveling in the direction of the open end of the crawler. The crawler horizontal square tube bumper support members that make contact with the storage cask are 1.85 m (73 inches) off the ground based on a telephone conversation with Lift Systems (crawler manufacturer).

Two bounding cases were evaluated for a drop of the storage cask onto the ISFSI concrete pad.

Case 1. A vertical drop without any rotation ("end drop")

Case 2. A drop causing maximum possible rotation.

For case 1, the calculation showed that the frictional resisting force of the storage cask sliding against the concrete was much less than the tip-over force and thus the storage cask would slide and not tip-over regardless of the velocity of the crawler. The maximum acceleration of the storage cask for an "end drop" case was calculated to be 44.13 g by Holtec (Reference A.1) assuming an 27.9 cm (11 inches) drop. This acceleration was increased by a factor of 1.045 to account for the 30.5 cm (12 inches) drop height being considered. This load factor was calculated using the Law of Conservation of Energy which equated the kinetic energy at impact to the work done in compressing the concrete pad and soil. Applying this load factor, the acceleration for the 30.5 cm (12 inches) drop was calculated to be 46.1 g. To obtain stresses for this end drop case use the stress results presented in the calculations for Question 10 (end drop case) and scale the results by the ratio 46.1 g / 60 g (= 0.768 factor).

For case 2, the calculation demonstrated that it is geometrically impossible for the rotation of the dropping storage cask to be large enough to cause a tip-over. The maximum amount of rotation possible is 5.14° (with respect to the ground) which occurs when one of the two vertical supports holding the storage cask at the top breaks and the cask makes contact with the ground at one edge. Since this angle is less than the "tip-over" angle of 29.5° (angle which would cause the storage cask to tip-over), the storage cask will not tip-over. Furthermore, the force required to tip-over the storage cask from the rotated orientation was calculated to be greater than the frictional resisting force. Therefore, the storage cask would slide but not tip-over. The acceleration and stresses under case 1 would also apply to this case.

In both cases, it is demonstrated that if the crawler has sufficient force, it would cause the storage cask to slide (not tip-over). However, if one object is pushing against another object (with both objects having the same coefficient of friction), the lighter object will slip or slide regardless of the magnitude of the coefficient of friction. Since the crawler weight is 71,440 kg (157,500 lb) and the storage overpack with MPC and fuel is 163,290 kg (360,000 lb), the crawler "tank treads" will slip and the storage cask will not slide or tip-over.

The drop of the storage cask onto an asphalt or gravel surface was also considered. The g values corresponding to this drop and the resulting stresses would be bounded by the drop onto the ISFSI concrete pad. This occurs because the asphalt and gravel have a lower strength and Young's modulus than concrete and both of these surfaces do not have steel reinforcing bars. Regarding sliding or tip-over, the same conclusion for the drop onto a concrete pad applies here that the crawler will slip and will not be able to slide or tip-over the storage cask. This assumes that both the crawler and storage cask are on the same surface (i.e., gravel or asphalt).

A.4.6.1 Refined Evaluations and Results for Question 6

Subsequently, refined calculations were performed for the 30.5 cm (12 inches) drop of storage cask onto the three surfaces; the asphalt, gravel, and ISFSI concrete pad. These refined nonlinear impact analyses were performed on the computer code LS-DYNA (Reference A.2) using existing computer models of the storage overpack obtained from Holtec International.

A.4.6.2 Storage Cask Drop onto Reinforced Concrete Storage Pad

A 30.5 cm (12 inches) vertical end drop of the storage cask impacting a 61 cm (24 inches) thick reinforced concrete pad, resting on soil was analyzed. Three analyses were performed corresponding to the lower bound, best estimate, and upper bound elastic soil modulii, which are equal to 324 MPa, 641 MPa, and 1,579 MPa (47,000 psi, 93,000 psi, and 229,000 psi), respectively. Poison's ratio is equal to 0.4 and the soil density is 2,003 kg/m^3 (125 lb/ft^3).

The maximum acceleration values for the 30.5 cm (12 inches) drop of the storage cask onto the 61 cm (24 inches) concrete pad resting on soil are shown in Table A.5.

The maximum acceleration at the bottom center of the storage cask is 41.2 g for the best estimate soil property. The acceleration time history at this location is shown in Figure A.32. The acceleration time history plot is initially flat at 1.0 g for a period of time because the storage cask was dropped from 30.5 cm (12 inches) height above the concrete pad and then impacted the pad at about 0.248 seconds. As shown in Table A.5, the variation in soil property does not have a significant effect on the maximum acceleration of the storage cask for the configuration and parameters defined for this load case.

Since the MPC shell was not discretely modeled, the stresses in the MPC were calculated using the stresses from Table A.6[Reference 9] for the end drop case and scaling the results in proportion to the new calculated g values.

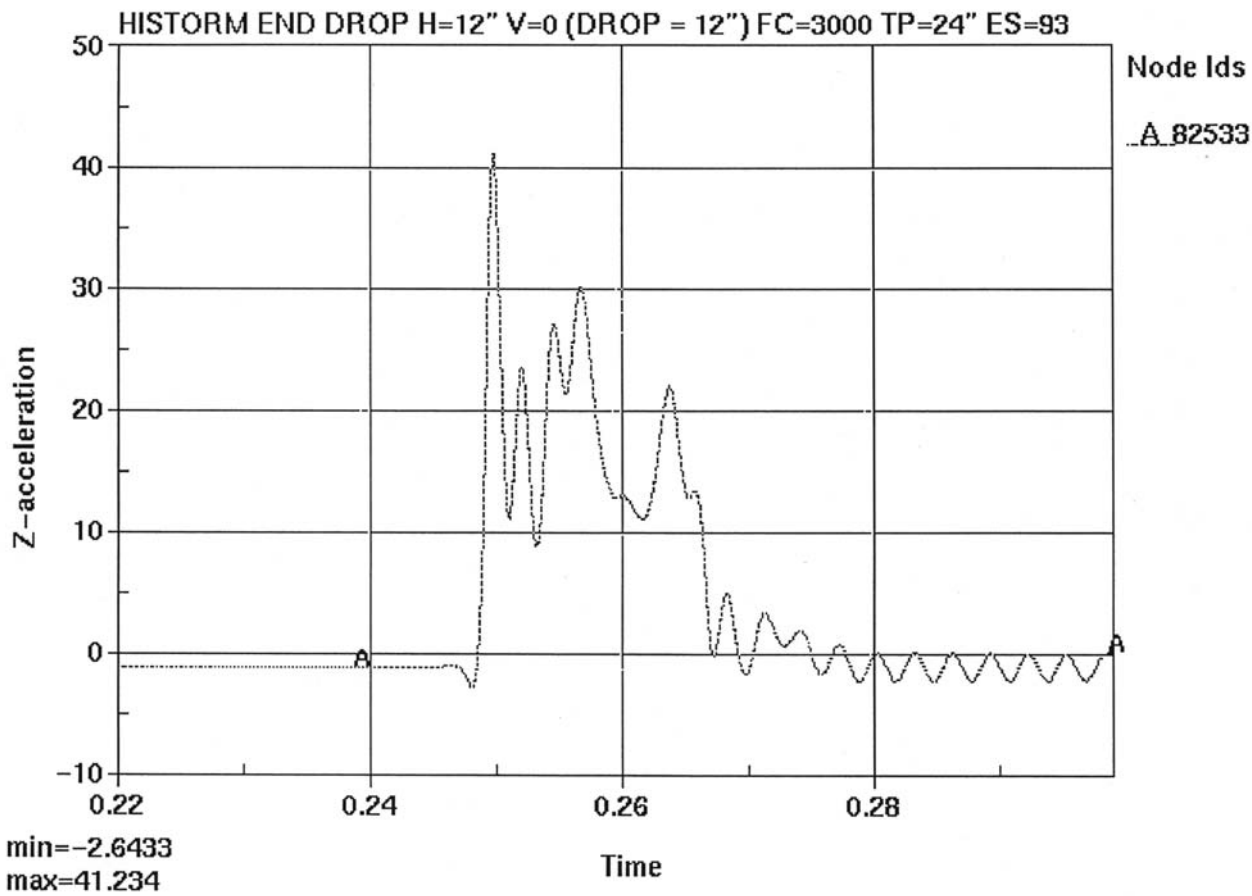

Figure A.32. Acceleration Time History - 30.5 cm (1 Ft) Drop on Concrete Pad

Table A.5. Storage Cask Drop Analyses

Impact Surface	Thickness of Target Layer (in)	Elastic Soil Modulus* (psi)	Maximum Acceleration (g)	Comment
Concrete	24	47,000	40.4	Lower bound soil property
	24	93,000	41.2	Best estimate soil property
	24	229,000	44.5	Upper bound soil property
Asphalt	12	93,000	25.4	Best estimate asphalt property at 4.4°C (40°F) and best estimate soil property
	12	93,000	23.2	Best estimate asphalt property at 23.9°C (75°F) and best estimate soil property
	12	93,000	Bounded by 23.9°C (75°F Case)	Best estimate asphalt property at 43.3°C (110°F) and best estimate soil property
Gravel	24	93,000	21.9	Best estimate gravel and soil properties
	12	93,000	15.8	Best estimate gravel and soil properties
	12	93,000	19.0	Upper bound gravel property and best estimate soil property

* Elastic soil modulus was based on the shear modulus calculated from the shear wave velocity of the free field

Using this approach and the appropriate dynamic load factor, the stresses in the MPC shell were calculated to be 53.3 MPa (7,732 psi). This stress value is well below the elastic buckling stress and yield for the MPC stainless steel material.

A.4.6.3 Storage Cask Drop onto Asphalt Surface

A 30.5 cm (12 inches) vertical end drop of the storage cask impacting a 30.5 cm (12 inches) thick layer of asphalt resting on soil was analyzed. Because asphalt material properties are sensitive to temperature, three loading cases were considered. The three cases correspond to material properties of asphalt at 4.4°C, 23.9°C, and 43.3°C (40°F, 75°F, and 110°F). This approximates the expected average temperature at the subject facility corresponding to winter, spring/fall, and summer. The properties for the asphalt layer were determined from a literature review of available information for a "good" asphalt mix. The best estimate values for the elastic modulus of asphalt are 10,342 MPa (1,500,000 psi) at 4.4°C (40°F), 4,482 MPa (650,000 psi) at 23.9°C (75°F), and 1,379 MPa (200,000 psi) at 43.3°C (110°F). At 4.4°C (40°F) the modulus of asphalt is approximately one-half the modulus of concrete.

Table A.6. MPC Stress Summary

Case	MPC Component	Drop Orien-tation	Safety Factor (SF)		Max. Stress (psi)	Direction/ Type of Stress	Acceleration (g)	Notes
			Value	Ref. A.1 Table #				
End Drop	Fuel Basket	Vertical	3.59[1]	3.4.3	-3,739	longitudinal	60	(A)
	Fuel Basket Support	Vertical			N.A.			(B)
	MPC Shell	Vertical	1.21	3.4.4	- 11,260	longitudinal	60	(C)
	MPC Lid	Vertical	2.8	3.4.4	± 2,723	bending	60	(D)
	MPC Baseplate	Vertical	1.28[2]	3.4.4	N.A.		60	(E)
Tip-over	Fuel Basket	45 Deg.	1.28[3]	3.4.3 & 3.4.6	± 38,335[4]	PL + Pb	45	(F)
	Fuel Basket Support	0 Deg.	1.18[5]	3.4.4 & 3.4.6	± 15,130[4]	direct + bending	45	(G)
	MPC Shell	0 Deg.	1.10	3.4.4	+ 58,959[4] - 45,283[4]	circum-ferential	45	(H)
	MPC Lid				N.A.			(I)
	MPC Baseplate				N.A.			(I)

Negative stress = compression, positive stress = tension
PL = Local membrane stress intensity; Pb = Primary bending stress intensity

1 SF of 3.59 is for lateral loading (not longitudinal)
2 Corresponds to ± 84.8 MPa (12,299 psi)
3 Corresponds to MPC-24
4 For tip-over case, stresses must be multiplied by a dynamic load factor of 1.04 (Ref. A.1)
5 Based on ANSYS Finite Element Model analysis

Notes column:
(A) Reference A.1, Sec. 3.4.4.3.1.3
(B) Basket support provides lateral not vertical restraint
(C) Reference A.21, App. 3.H Case 5 - Buckling
(D) Reference A.21, App. 3.E.8.2.1.1
(E) MPC baseplate supported by storage overpack baseplate.
(F) Reference A.1, App. 3.T.32
(G) Reference A.1, App. 3.Y.3 for MPC-68
(H) Reference A.1, App. 3.T.34; includes stress due to D.W. & internal pressure (σ of +47.1 MPa (+6,838 psi))
(I) Bounded by End Drop Case

The maximum acceleration values for a 30.5 cm (12 in.) drop of the storage cask for the 4.4°C and 23.9°C (40°F and 75°F) are shown in Table A.5. The 43.3°C (110°F) drop case was not analyzed because at this high temperature, the acceleration would be lower than the 23.9°C (75°F) case. The maximum accelerations at the bottom center of the storage cask, for the best estimate asphalt property are 25.4 g and 23.2 g for the 4.4°C and 23.9°C (40°F and 75°F) cases, respectively.

The stresses in the MPC were calculated using the stresses from Table A.6 for end drop case and scaling the results in proportion to the new calculated g values. Using this approach and the appropriate dynamic load factor, the vertical stresses in the MPC shell were calculated to be 50.0 MPa (7,245 psi) and 45.6 MPa (6,618 psi) for the 4.4°C and 23.9°C (40°F and 75°F) cases, respectively. Both of these stress values are well below the elastic buckling stress and yield for the MPC stainless steel material.

A.4.6.4 Storage Cask Drop onto Gravel Surface

Two cases were considered for the storage cask drop on a gravel surface. A 30.5 cm (12 inches) vertical end drop of the cask impacting a 30.5 cm (12 inches) and 61 cm (24 inches) thick gravel layer resting on soil was evaluated. The 61 cm (24 inches) layer corresponds to the gravel region surrounding the concrete pad where the storage casks are stored, while the 30.5 cm (12 inches) layer corresponds to the gravel region away from the concrete pad where the gravel layer tapers to smaller thicknesses. The properties for the gravel layer were determined from a literature review of available information on "well graded" crushed stone aggregate. The best estimate value of 345 MPa (50,000 psi) for the elastic modulus would tend to be somewhat higher than what might be expected at the subject facility. This would be conservative because a higher modulus would result in higher impact forces and accelerations. To gauge the effect of varying the modulus of the gravel material, an analysis was performed for the best estimate value 345 MPa (50,000 psi) and for the upper bound estimate 689 MPa (100,000 psi) for the 30.5 cm (12 inches) thick gravel layer case.

The maximum acceleration values for a 30.5 cm (12 in.) drop of the storage cask onto the 61 cm and 30.5 cm (24 inches and 12 inches) gravel layers are shown in Table A.5. The maximum accelerations at the bottom center of the storage cask, for the best estimate gravel property are 21.9 g and 15.8 g for the 61 cm and 30.5 cm (24 inches and 12 inches) gravel layer cases, respectively. As a measure of the sensitivity of the gravel material property, an upper bound case for the gravel property was performed for the 30.5 cm (12 inches) gravel layer. The maximum acceleration for this upper bound gravel property was 19.0 g.

The stresses in the MPC were calculated using the stresses from Table A.6 for end drop case and scaling the results in proportion to the new calculated g values. Using this approach and the appropriate dynamic load factor the vertical stresses in the MPC shell, for the 30.5 cm (12 inches) drop case, were calculated to be 39.7 MPa (5,754 psi) and 28.6 MPa (4,151 psi) for the 61 cm (24 inches) and 30.5 cm (12 inches) gravel layers, respectively. Both of these stress values are well below the elastic buckling stress and yield for the MPC stainless steel material.

A.4.7 Question 7

If the crawler vehicle weighing 71,440 kg (157,500 lb) is traveling at 0.64 km/h (0.4 mi/h) while carrying the storage cask weighing 163,293 kg (360,000 lb), hits another storage cask on a concrete pad, will this impact slide or tip-over the "struck" cask?

(A) If it slides, will a sliding storage cask hit another storage cask? If it hits another storage cask, what would be the maximum stresses (e.g., axial, circumferential, tensile, and compressive) in the MPC?

(B) If it tips over, what would be the maximum stresses in the MPC?

(C) If it does not slide or tip-over, what travel velocity of the crawler would be necessary to strike the storage cask and cause it to slide and/or tip-over?

The evaluation first determined whether a horizontal force would cause the storage cask to tip-over or slide. For tip-over, a horizontal force of 149,732 kg (330,103 lb) applied at 1.85 m (73 inches) off the ground would be needed. This dimension off the ground corresponds to the height of the horizontal square tube bumper supports on the crawler. These supports show up on the photos and Lift System drawings and this dimension was confirmed by Lift Systems (crawler manufacturer). The force needed to overcome friction ranges from 40,823 kg (90,000 lb) for minimum coefficient of friction of 0.25 to 86,545 kg (190,800 lb) for maximum coefficient of friction of 0.53. For the range of coefficient of friction used see Question 8. Since the force necessary to overcome friction is much lower than the force needed to cause tip-over, the struck cask will slide and not tip-over.

Since the struck cask will slide, only Part (A) of Question 7 is applicable. The initial velocity of the struck cask was calculated using the principle of Conservation of Momentum. This led to the initial velocity of the struck cask to be:

$$x'_0 = \frac{mV}{\left(m + \frac{W}{g}\right)} \qquad (A.8)$$

where: m = mass of crawler + mass of storage cask being transported
V = velocity of crawler
W = weight of storage cask

When the crawler carrying the storage cask strikes another storage cask, the resulting velocity will be reduced. The calculated resulting velocity x'_o of the combined crawler, storage cask being transported, and struck storage cask is 0.38 km/h (0.24 mi/h).

The equation of motion of the storage cask after impact is:

$$M_3 x'' + \mu W - F_c = 0 \qquad (A.9)$$

where: M_3 = mass of crawler + 2 storage casks
F_c = horizontal force that the crawler can generate, 139,603 kg (307,772 lb) [1]

The solutions for velocity and displacement are found by integrating Equation A.10 and evaluating the two constants of integration from the initial velocity of Equation A.9 and zero initial displacement. Equations A.11 and A.12 for velocity and displacement are:

$$x' = \left(\frac{F_c - \mu W}{M_3}\right) t + \frac{m\,V}{\left(m + \frac{W}{g}\right)} \qquad (A.10)$$

1 / Source: Lift Systems Spec. Sheet & confirmed by telephone discussion with C. Perkins of Lift Systems

$$x = \left(\frac{F_c - \mu W}{M_3} \right) \frac{t^2}{2} + \frac{m\ V}{\left(m + \frac{W}{g} \right)} t \qquad (A.11)$$

The maximum displacement occurs when the velocity equals zero and is found to be:

$$x = \left[\frac{1}{2\left(\frac{\mu\ W - F_c}{M_3} \right)} \right] \left[\frac{m\ V}{m + \frac{W}{g}} \right]^2 \qquad (A.12)$$

This equation tells us that as the value F_c approaches μ W, the displacement goes to infinity. By inserting the appropriate numbers, F_c is calculated to be greater than μ W. Therefore, it is concluded that the crawler will continually push the storage cask. The sliding storage cask will eventually hit another storage cask or slide off the pad onto the surrounding area. This assumes that the crawler does not stop but continues pushing the struck cask.

Part (A) of Question 7 also asks, what would be the maximum stresses in the MPC? Equation A.10 can be used to determine the acceleration of the storage cask. Solving for x" provides the acceleration as:

$$x'' = (F_c - \mu\ W) / M_3 = 0.25\ g$$

Therefore, the maximum acceleration of the storage cask would be 0.25 g. The positive value of acceleration indicates that the storage cask would accelerate under the constant force (not decelerate). The maximum stresses in the MPC could be approximated by multiplying the stresses presented in the calculations for Question 10 for the tip-over case by the ratio of accelerations 0.25g / 45g for the fuel basket, basket supports, and the MPC shell. For the MPC lid and baseplate, the end drop case bounds and the stresses would be multiplied by 0.25g / 60g. Note that there is also the dynamic load factor of 1.04 to be applied to the tip-over case (see calculations for Question 10).

A.4.8 Question 8

What seismic forces will cause the storage cask to slide and/or tip-over?

A.4.8.1 Simplified Seismic Evaluation

Simplified analyses without soil structure interaction were performed for a storage cask (containing a fully loaded MPC-68) subjected to earthquake forces. The storage cask was assumed to be resting on the ISFSI concrete pad. The seismic analyses used the equivalent static load method which simply multiplies the mass times the seismic equivalent static acceleration to arrive at the seismic forces. To determine whether any amplification occurs due to the flexibility of the storage cask, the natural frequency of the storage cask was calculated. The fundamental frequency of the storage cask was calculated to be well above 20.6 Hz

which is above the amplified region of the ground spectra or the spectra that would exist on the ISFSI concrete pad. The storage cask frequency was calculated by treating the inner and outer steel cylindrical shells of the storage overpack as cantilever beams fixed at the base. Conservatively, the stiffness contribution of the concrete inside the overpack and the MPC shell was not included. The calculation considered flexural and shear effects in calculating the beam frequency. The seismic analysis also assumed no amplification due to soil-structure interaction. Based on the above discussion, the use of the equivalent static method without any amplification would be appropriate and the resulting acceleration calculated for sliding and tip-over would correspond to the maximum ground acceleration.

Two cases are considered in this evaluation, a 3 Dimensional (3 D) earthquake (2 horizontal and 1 vertical) and a 2 Dimensional (2 D) earthquake (1 horizontal and 1 vertical). Both are being considered because the subject plant FSAR indicates that the three directional responses are combined by the square-root-of-sum-of-squares method or by the absolute sum of the worst horizontal with the vertical. The vertical acceleration is assumed for this calculation to be equal to 2/3 of the horizontal acceleration. This is consistent with most nuclear power plants in the U.S. and is consistent with the subject plant FSAR.

To determine whether seismic forces cause sliding or tip-over, the seismic force that would initiate sliding was calculated and compared to the force needed to cause tip-over of the storage cask. Sliding would occur when the seismic force exceeds the frictional resistance of the storage cask due to dead weight. The frictional resistance (F_f) is defined in Equation A.13.

$$F_f = \mu N \qquad (A.13)$$

where: μ = coefficient of friction between steel and concrete
N = dead weight of the fully loaded storage cask

Since the coefficient of friction varies, a range of values for μ was utilized as follows:

- μ (minimum) is 0.25, based on a conservative value (for lower bound) in Reference A.1, Section 3.4.6 & 3.4.7.
- μ (maximum) is 0.53, based on Reference A.12, Section 3.4.
- μ (mean) is 0.43, based on Reference A.13. This paper presents results of tests conducted with anchored baseplates which confirm that the range of μ shown above is reasonable and also indicates that the standard deviation of μ is 0.09.

Using these coefficients of friction for a 3 D and 2 D earthquake, the seismic forces, in terms of individual horizontal acceleration, that would cause sliding are calculated. To obtain the corresponding vertical accelerations, the horizontal accelerations are multiplied by 2/3. The resulting governing case (sliding) is presented in Table A.7 for the 2-D and 3-D earthquake cases.

Horizontal acceleration required for tip-over was calculated to be 0.529 g for 3-D case, and 0.410 g for 2-D case. Since the accelerations shown in Table A.7 are less than the accelerations that would cause tip-over, it was concluded that the storage cask would slide and not tip-over.

Table A.7. Seismic Maximum Accelerations for Sliding

Coefficient of Friction μ	2 - D Earthquake Plant	3 - D Earthquake Plant

	Horizontal Acceleration For Sliding (g)	Vertical Acceleration (g)	Horizontal Acceleration For Sliding* (g)	Vertical Acceleration (g)
0.25 (min)	.214	.143	.243	.162
0.43 (mean)	.334	.223	.413	.275
0.53 (max)	.392	.261	.50	.333

* For the 3 D earthquake, the horizontal accelerations correspond to each of the two orthogonal directions. It should be noted that these two peak accelerations would not occur at the same time which is accounted for in the square-root-of-sum-of-squares method used in this calculation.

A.4.8.2 Refined Seismic Evaluation

Calculations for the seismic question were independently done with the consideration of soil-structure interaction:

A three-dimensional coupled finite element model of a cylindrical storage cask, a flexible concrete pad, and an underlying soil foundation was analyzed using the ABAQUS/Explicit code, (Reference A.14). The cylindrical storage cask is partitioned into four horizontal sections with six rows of solid elements in each section and 64 elements around the outside perimeter. The density of solid elements in each horizontal section is calculated and distributed in such a manner that the center of gravity of the storage cask is located at the correct design position. The storage cask and its internals are modeled as elastic bodies.

In the coupled model, the base of the concrete pad was assumed rigidly bonded to the top surface of the soil foundation. At the storage cask/pad interface, a sliding contact condition was assumed with an assigned friction coefficient of 0.25, or 0.53. The top of the pad was designated to be the "master" surface and the underside of the module to be the "slave" surface to prevent any portion of the module from entering the pad. The four vertical sides of the soil foundation were represented by edge columns that allow horizontal shear deformation only in order to simulate infinite boundary conditions. The earthquake excitation information was treated with a deconvolution procedure to produce a modified time history of deconvoluted accelerations with properly adjusted frequencies and magnitudes to be applied at the base of soil foundation. The concept of deconvolution is a mathematically rigorous solution process that applies the wave propagation equation of the free-field surface along with the boundary conditions. It has been proven that the solution would be unique and rigorously correct for a linear representation of the soil mass (that is, linear shear modulus and viscous damping model). The deconvolution procedure has been discussed in References A,15 and A.16. The input motions of deconvoluted seismic accelerations were applied to all nodes at the base of the soil foundation. The following data for the storage overpack with MPC-68 fully loaded with fuel was used.

- Weight = 163,293 kg (360,000 lb)
- Outside Diameter = 3.37 m (11.04 ft)
- Height = 5.87 m (19.27 ft)
- Height of center of gravity above pad = 3.00 m (9.86 ft)

A section of the concrete pad that holds 4 (2x2) storage casks was selected as the optimal dimension for the pad in the coupled model, even though only one storage cask was simulated. The selected pad was 9.45 m (31 ft) square. The pad thickness was 0.61 m (2 ft).

The size of soil foundation model plays an important role in assessing the soil-structure-interaction effect. Sensitivity studies on the size were performed to demonstrate that its chosen model size could simulate the behavior of a semi-infinite soil foundation underneath the concrete pad. Three different lateral dimensions were selected having 1.0, 1.22, and 1.33 times a baseline lateral geometry of a square of 85 m (279 ft), which is nine times the pad dimension. It should be noted that the outside layer of elements on the four vertical sides of soil foundation model, with width equal to the pad dimension of 9.45 m (31 ft), are represented by edge columns. This model setup indicates that the true model size is defined by the nodes at the inner row of the layer with degrees of freedom constrained to those at the outside row. Therefore, the baseline geometry of soil foundation model is only seven times the pad dimension. This selection of the lateral dimension of soil foundation model follows the soil-structure-interaction modeling guidelines in Reference A.17.

The sensitivity studies on the model sizes for the horizontal displacements of the storage cask base with respect to the pad showed closer displacement solutions for the cases of 1.22 and 1.33 times the baseline geometry, indicating that a convergence trend of soil foundation model sizes was observed. Therefore, the final soil foundation model, which was selected to be 1.22 times the baseline geometry, was a square with length of 103.94 m (341 ft). In addition, a depth of 56.39 m (185 ft) which was partitioned into eight horizontal layers was selected for soil foundation model.

The storage cask and the concrete pad are assumed to behave elastically when subjected to seismic excitations. Therefore, their elastic material properties were chosen as shown in Table A.8.

Table A.8 Elastic Material Properties of Storage Cask and Pad

Structural Element	Young's Modulus, E (MPa) (x 103)	Poisson's Ratio, n	Density, r (kg/m3)
Storage cask	27.789	0.2	6408 (Section 1)*
			2600 (Section 2)*
			2600 (Section 3)*
			3407 (Section 4)*
Pad	24.856	0.2	2403

The geometric definitions of the horizontal sections are as follows.

* Section 1: from storage cask base to 0.2 m (8 inches) above base
* Section 2: from 0.2 m (8 inches) above base to 0.6 m (2 ft) above base
* Section 3: from 0.6 m (2 ft) above base to 3 m (9.86 ft) above base
* Section 4: from 3 m (9.86 ft) above base to storage cask top

The 56.39 m (185 ft) depth of soil foundation model is partitioned into eight horizontal layers. The depth variation of soil properties such as shear wave velocity and damping profiles was developed to incorporate the site specific soil profiles. The best-estimated strain-compatible soil properties were selected to be used in the seismic analyses. The weight density of the top 56.39 m (185 ft) of soil foundation was estimated to be 2,162 kg/m^3 (135 lb/ft^3).

The final seismic analyses used the mass proportional soil damping, x_n for each layer such that

$$\xi_n = \frac{a_0}{2\omega_n} \text{ where } a_0 = 2\xi * \frac{2\pi}{T} \qquad (A.14)$$

For shear wave propagation model of horizontal motion site response, site period T is assumed as 0.53 second. For compression wave propagation model of vertical motion site response, site period T is assumed as 0.33 second.

The time history utilized was the one used by the applicant for the design basis. The selected PGA level is 0.15 g for the two horizontal directions and 0.1 g for the vertical direction. Two horizontal components and one vertical component of the seismic accelerations, which are "surface" motions, were applied simultaneously to the coupled model. A frequency domain deconvolution procedure was applied to the time histories of seismic surface accelerations. This procedure uses the Fourier transforms to adjust simultaneously their magnitudes and frequency contents. The net outcome is that when deconvoluted seismic motions are applied at the base of soil foundation model, the dynamic characteristics of the original seismic motions is preserved and the desired surface shaking intensity can be achieved.

For seismic excitation analyzed with horizontal PGA of 0.15g, and vertical PGA of 0.1g using 3-D coupled nonlinear finite element model of the storage cask, pad and soil underneath, the analyses show that the storage cask may slide less than 0.1" assuming lower bound coefficient of friction 0.25, and will not tip-over with any coefficient of friction from 0.25 to 0.53.

Sensitivity analyses were then performed for different level of seismic excitations with different coefficients of friction between the bottom steel plate of the storage overpack and the concrete pad using three-dimensional coupled finite element models of the cylindrical storage cask, a flexible concrete pad, and an underlying soil foundation. When higher levels of seismic excitations are used in the analyses, the coefficient of friction at the storage cask/pad interface plays an increasingly important role in the sliding and rotational behavior of the storage cask. For a minimum friction coefficient, the storage cask exhibits a translational motion without much rotation. When the friction coefficient is 0.25, eleven times the design-basis earthquake of the ISFSI pad (i.e., 11 DBE) is needed to cause the storage cask to slide 0.93 m (36.6 inches); this is more than half the separation distance of 1.36 m (53.5 inches) between neighboring casks. For a maximum friction coefficient, the storage cask experiences more rotational movement, but not tip-over. When the friction coefficient is 0.53 and the seismic excitations are increased to nine times the design-basis earthquake (i.e., 9 DBE), the neighboring storage casks may collide as the cask top moves 1.19 m (46.7 inches) and the cask base slides 0.84 m (33.1 inches). In these cases, the storage cask will slide but not tip-over. Collision may occur at the seismic excitation level of 9 DBE or higher. This level of earthquake is so high in intensity that the plant may have serious consequences, and the consequences due to casks collision will be of no significance compared to the plant.

A.4.9 Question 9

What impact forces due to given small aircraft, tornado missiles (beyond design basis) and heavy objects in flood waters will cause the storage cask to slide and/or tip-over? If an object of such an impact penetrates the storage overpack, what would be the stresses in the MPC?

The aircraft impact to be evaluated is from a small, non-commercial aircraft, Gulfstream IV, accidentally hitting the storage cask either by a free fall or with its engine running.

The tornado missiles to be considered are the Spectrum II missiles identified in Reference A.18. The calculations below use the tornado missile which most likely will cause the storage cask to slide/tip and/or penetrate the storage overpack and strike the MPC. If this initial analysis shows no penetration or negligible stresses in the MPC, less severe missiles need not be evaluated; otherwise, analyze them in the order of severity (i.e., the most severe one first).

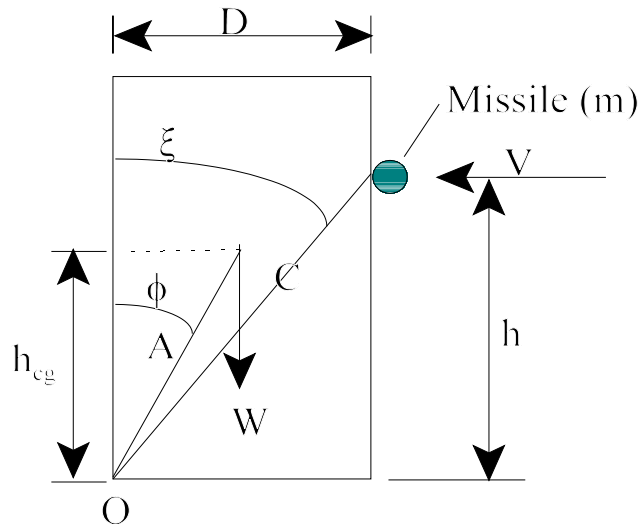

Figure A.33. Tip-over of Storage Cask

A.4.9.1 Missile Impact Analysis

This calculation addresses the effects of the missiles impact such as automobile and aircraft crashing into the storage overpack. The missile and storage cask are assumed to be rigid. Missile impact on the storage cask can result in either tip-over or sliding the storage cask. The tip-over and sliding modes are considered independently and it is assumed that the storage cask either slides or tips over with no interaction between the two response modes. An approach is first developed to evaluate the effects of any type of rigid missile impact. Then, this approach is used to analyze the impact due to an automobile and small aircraft crash.

A.4.9.1.1 Tip-over Due to Missile Impact

The tip-over mode is considered first. Consider the storage cask with the configuration shown in Figure A.33. A missile of mass (m) and velocity (V) impacts the storage cask at a distance (h) above the base. The horizontal velocity of the missile is first converted to an angular velocity (ω_m) about point (O) by:

$$\omega_m = \frac{V \cos\xi}{C} \qquad (A.15)$$

Conservation of momentum results in a combined angular velocity of the storage cask and missile equal to:

$$\omega = \frac{m\,C\,V\,\cos\xi}{\left(\frac{WA^2}{g} + m\,C^2\right)} \qquad (A.16)$$

Conservation of energy principles are then used to determine the initial angular velocity (ω_c) required to tip-over when the center of gravity is directly above point O:

$$\omega_c^2 = \frac{2\left[W\,A\left(1-\mathrm{Cos}\phi\right)+m\,g\;C\left(1-\mathrm{Cos}\;\xi\right)\right]}{\left(\frac{WA^2}{g}+mC^2\right)} \qquad (A.17)$$

Combining Equations A.16 and A.17 and solving for (V) results in:

$$V^2 = \frac{2\left[WA\left(1-\mathrm{Cos}\;\phi\right)+m\,g\,C\left(1-\mathrm{Cos}\,\xi\right)\right]\left[\frac{W\,A^2}{g}+m\,C^2\right]}{\left(m\,C\;\mathrm{Cos}\,\xi\right)^2} \qquad (A.18)$$

A spreadsheet is then used to evaluate (V) given a missile mass (m)

where:

W	=	163,290 kg (360,000 lb)
D	=	3.4 m (133.875 inches)
h_{cg}	=	3 m (118.4 inches)
ϕ	=	29.5º
A	=	3.45 m (136 inches); $C = (h^2 + D^2)0.5$
ξ	=	$\tan^{-1}$ (D/h); the value of (h) is taken as 1 , 0.75, 0.5, and 0.25 times the height of the storage cask= 5.87 m (231.25 inches)

The resulting velocities required to tip-over the storage cask are shown in Figure A.34.

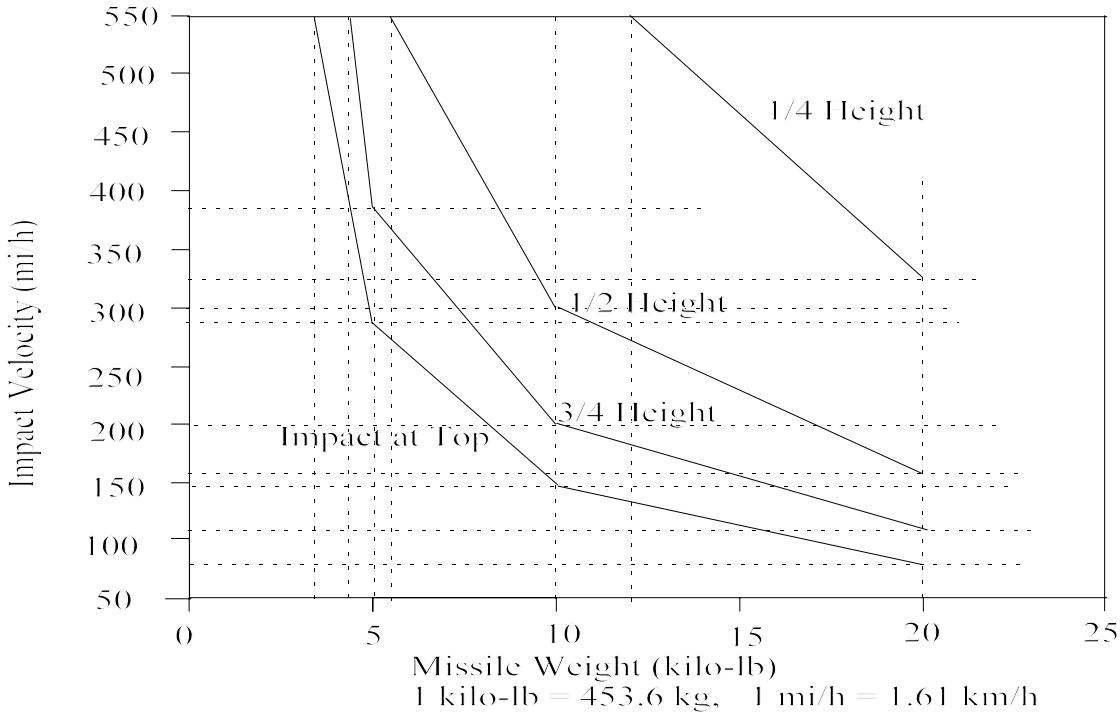

Figure A.34. Missile Velocity for Tip-over of Storage Cask

A.4.9.1.2 Sliding Due to Missile Impact

Sliding of the storage cask is considered next. A sketch of the problem is shown in Figure A.35.

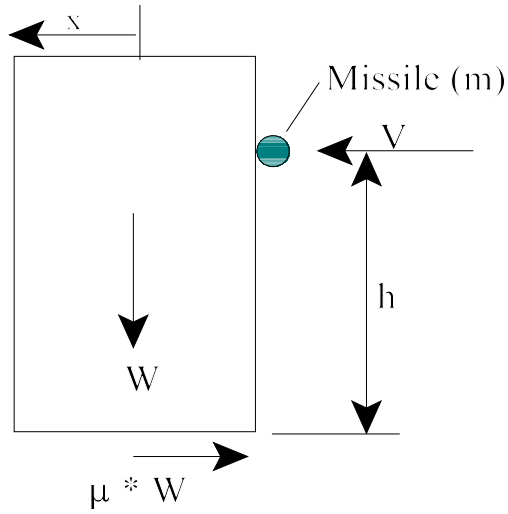

Figure A.35. Sliding of Storage Cask

The height of the missile impact is not important for this problem, because here we are concerned with the sliding mode only. Conservation of momentum results in the following initial velocity (x'_o) of the storage cask after impact:

$$x'_0 = \frac{m\,V}{\left(m + \frac{W}{g}\right)} \qquad (A.19)$$

The equation of motion for the storage cask after impact is:

$$x'' + \mu\, g = 0 \qquad (A.20)$$

Integrating Equation A.20 and evaluating the two constants of integration from the initial velocity of Equation A.19 and zero initial displacement results in the following solutions for velocity and displacement:

$$x = \frac{m\,V\,t}{\left(m + \frac{W}{g}\right)} - \frac{\mu\, g\, t^2}{2} \qquad (A.21)$$

where t = time after impact

The maximum displacement occurs when the velocity equals zero and is found to be:

$$x' = \frac{m\,V}{\left(m + \frac{W}{g}\right)} - \mu\, g\, t \qquad (A.22)$$

$$x_{max} = \frac{\left(\frac{m\,V}{\left(m + \frac{W}{g}\right)}\right)^2}{2\,\mu\, g} \qquad (A.23)$$

The clear spacing between the storage casks on the ISFSI pad is at least 1.3 m (52.1 inches) and the closest clear distance from the edge of the storage cask to the edge of the pad is 66 cm (26 inches). Solutions are therefore obtained for x_{max} = 66 cm (26 inches). Three values of the coefficient of friction are used (see calculations for Question 8); a lower bound of 0.25, a mean value of 0.43, and an upper bound of 0.53. Equation A.23 is solved for the velocity required to slide the storage cask 66 cm (26 inches) given the missile mass. These solutions are shown in Figure A..36.

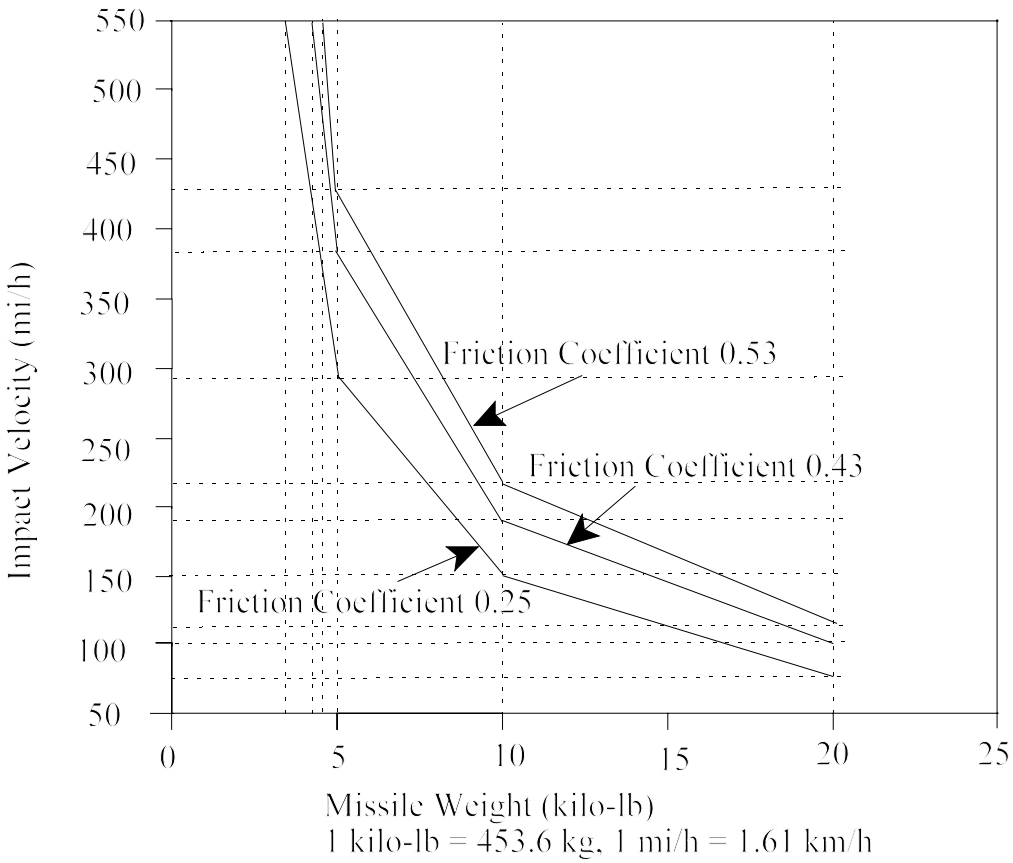

Figure A.36. Missile Velocity Required to Slide the Storage Cask by 66 cm (26 inches)

The following conclusions can be drawn by comparing Figures A.34 and A.36:

A) Impact velocities required to cause the storage cask to slide are about the same as those required to cause it to tip-over if the coefficient of friction = 0.25 and the impact is at the top of the storage cask. The storage cask will slide rather than tip-over if the impact is below the top of the cask and the friction coefficient = 0.25.

B) The storage cask will tip-over rather than slide if the friction coefficient = 0.43 and the impact height is larger than about 80 % of the height. It will slide if the impact is below this height.

C) The storage cask will tip-over rather than slide if the friction coefficient = 0.53 and the impact height is larger than about 62.5 % of the height. It will slide if the impact is below this height.

A.4.9.2 Vehicle Impact

A car or a truck crashing into the storage casks while stored on the ISFSI pad is not analyzed directly for a driver's accidental maneuver, physical ailment or mistake. However, by extrapolation from the analyses done for tip-over and sliding due to missile impact (from Figures A.34, 35, and 36 respectively), it can be concluded that a 4,536 kg (10,000 lb) vehicle traveling at 241 km/h (150 mi/h) speed will slide the storage cask less 66 cm (26 inches), and will not cause tip-over. This conservatively assumes that the impact occurs at the top of the storage cask (for tip-over) and the lowest coefficient of friction applies (for sliding).

A.4.9.3 Aircraft Impact Analysis

The analyses described below are included in this Appendix to provide a methodology for determining the response of a dry storage cask to aircraft impact. The results of the aircraft impact analyses are used in the PRA to evaluate aircraft impact events on overall risk.

As discussed in Section 3.3.7 of the main report, the largest aircraft that is able to land at any of the four local airfields near the ISFSI site is a Gulfstream IV. This aircraft's geometric characteristics were used to estimate the frequency of an aircraft crash into a storage cask during takeoff or landing. The data and equations presented in Sections A.4.9.3.1 and 2 are used to evaluate the global and local structural response of a storage cask to impact by a Gulfstream IV. Section A.4.9.3.3 summarizes the results and discusses the probability of breaching the MPC confinement boundary.

A.4.9.3.1 Global Response

The Gulfstream IV aircraft weighs 74,600 lbs on takeoff and is powered by two Roll-Royce Tay 611-8 turbofan jet engines each weighing 3,135 lbs. The DOE Standard on aircraft impact (Reference A.19) recommends that the gross response of a target can be evaluated by considering the impact of a rigid missile having a mass equal to twice the engine weight. Thus the appropriate missile weight for the analysis is 2 x 3,135 = 6,270 lbs. Figures A.34 and A.36 are used to obtain the impact velocity required for tip-over and sliding. The results are shown in Table 9a.

Table A.9a. Global Response of Storage Cask to Aircraft Impact

Tip-over		Sliding	
h/L	Impact Velocity Required (mph)	μ	Impact Velocity Required (mph)
1	250	0.25	260
0.75	340	0.43	330
0.5	500	0.53	370

A.4.9.3.2 Local Response

Another mode of response to missile impact is local penetration or perforation of the shell and lid of the storage overpack. The DOE Standard (Reference A.19) recommends that the local damage evaluation be performed using relatively nondeformable components of the aircraft. Such a component is the engine shaft. The Rolls-Royce Tay 611-8 engine is 94.8 inches long and 45.0 inches in diameter. Exact dimensions of the engine shaft were not available from the manufacturer, so dimensions were estimated from available photographs and cross sections of jet engines of this class.

A typical turbofan engine has multiple concentric shafts, but for the purpose of this analysis a single solid shaft is assumed. The shaft is assumed to have an average diameter of 4.0 inches over 80% of the engine length. The resulting weight of the shaft is (π x 2^2 x 94.8 x 0.80 x 490/1728 = 270) 270 lbs.

The shell of the storage overpack consists of an outer steel shell 0.75 inches thick, a poured concrete shell 26.75 inches thick and an inner steel shell 1.25 inches thick. The lid consists of a top steel plate 2.0 inches thick, a bottom steel plate 2.0 inches thick, a concrete shield plug 10.5 inches thick and a bottom shield plate 1.25 inches thick.

The DOE Standard on aircraft impact analysis (Reference A.19) recommends the Chang formula (Equation 24a) to compute the perforation thickness of concrete targets and the Ballistic Research Laboratory (BRL) formula (Equation A.24b) to compute the penetration thickness of steel targets.

$$t_p = \left(\frac{U}{V}\right)^{0.25} \left(\frac{M V^2}{D f_c'}\right)^{0.5} \qquad \text{(A.24a)}$$

where:

U = reference velocity = 200 ft/sec;
V = missile impact velocity (ft/sec);
M = mass of the missile = W/g,
W = missile weight (lb), g=32.2 ft/sec^2
D = effective missile diameter (ft);
f'c = ultimate compressive strength of concrete (lb/ft^2);
t_p = mean perforation thickness (ft).

$$T^{1.5} = \frac{0.5MV^2}{17{,}400K_s D^{1.5}} \tag{A.24b}$$

where

T = predicted thickness to just perforate a steel plate (in.);
M = W/g missile mass (lb-sec^2/ft);
V = missile impact velocity (ft/sec);
K_s = constant depending on the grade of steel (usually ≈ 1);
D = missile diameter (in.).

Both formulae in their standard form assume the missile is rigid. To prevent perforation of the target, Reference A.19 recommends that the thickness computed using the Chang and BRL formulae be reduced by a factor of 1.2 and 1.25 respectively.

The storage overpack shell and lid consist of multiple layers of steel and concrete. The approach used to determine the impact velocity that will just perforate all the layers of the storage overpack shell and lid is to separately calculate the kinetic energy associated with the impact velocity required to just perforate each of the steel and concrete layers, and then add the kinetic energies from each layer to determine the total kinetic energy and resulting impact velocity. This methodology is based on the conservative assumption that each layer behaves independently and that there is no interaction between layers. Since multiple layers resist perforation, it would be overly conservative to reduce the thickness of each layer by the reduction factors cited above, because these factors are intended to prevent perforation. To establish a realistically conservative best estimate of the impact velocity that will just perforate all the layers, only the layer contributing most to perforation resistance is reduced in thickness.

For each storage overpack shell and lid layer, Table A.9b shows the material and thickness of the layer, the reduced thickness, the kinetic energy required to just perforate the layer, the total kinetic energy from all layers and the resulting impact velocity of the aircraft. This methodology produces conservative results. More accurate results can be obtained using explicit dynamics found in several commercially available computer codes. Before using such codes, however, material models, elements and meshes should be benchmarked against the results of actual test data.

Table A.9b. Aircraft Maximum Impact Velocity that Does Not Perforate the Storage Overpack Shell or Lid.

Event	Target Layer	Thickness (in)	Reduced Thickness (in)	Kinetic Energy to Perforate (ft-lbs)	Total Kinetic Energy (ft-lbs)	Maximum Impact Velocity(1) (mph)
Horizontal Impact into Overpack Shell	Outer Steel Shell	0.75	0.75	(3)	(3)	(3)
	Concrete Shell	26.75	22.30	(3)		
	Inner Steel Shell	1.25	1.25	(3)		
Vertical Impact into Overpack Lid	Top Lid Plate	2.00	2.00	(3)	(3)	(2)(3)
	Bottom Lid Plate	2.00	1.60	(3)		
	Shield Concrete	10.5	10.5	(3)		
	Bottom Shield Plate	1.25	1.25	(3)		

(1) The methodology used here produces conservative results. More accurate results can be obtained using explicit dynamics found in several commercially available finite element computer codes. Before using such codes, material models, elements and meshes should be benchmarked against the results of impact test data.
(2) Assumes an impact angle of 50 degrees above the horizontal.
(3) Text withheld under 10 CFR 2.390.

A.4.9.3.3 Results of Aircraft Impact Analysis

Aircraft speeds during landing and takeoff generally range from 140 to 200 mph (Reference A.19). Table A.9a shows that cask tip-over or sliding due to aircraft impact would not be expected to occur until impact speeds exceed 250 mph, and then, only if the aircraft struck near the top of the cask. The response of the MPC to cask tip-over is far more significant than to cask sliding, and therefore only cask tip-over need be considered. As reported in Table B.6, the probability of MPC failure due to cask tip-over is less than $1x10^{-6}$. Table A.9b shows that perforation of the storage overpack would not occur until impact speeds exceed (text withheld under 10 CFR 2.390). For the largest aircraft that can land or takeoff from any of the four airports near the site, these results show that the storage overpack provides a rugged barrier that makes the likelihood of an MPC breach from aircraft impact exceedingly small.

Based on these results, the probability of breaching the MPC, if struck by an aircraft during landing or takeoff is extremely small and is assumed to be zero. However, many commercial aircraft overflying the site would be larger than a Gulfstream IV and could impact the cask at velocities much higher than those associated with landing and takeoff. Since the makeup and

characteristics of commercial aircraft overflying the site are not known, and have not been evaluated, it is conservatively assumed that all commercial aircraft overflying the site are larger than a Gulfstream IV and that the probability of MPC breach due to the impact of an overflying commercial aircraft is, for the purpose of the PRA, 1.0. Therefore, the probability of MPC failure and release, if struck by an aircraft, is, for the purpose of the PRA, equal to the frequency of overflight crashes (5.1×10^{-10}, see Section 3.3.7) divided by the total frequency of aircraft crashes (3.71×10^{-9}, see Section 3.3.7), which is 0.14.

A.4.9.4 Tornado Missile Impact Analysis

This calculation considers the local effects of tornado missiles hitting the storage cask and addresses the question of whether the missiles penetrate the storage overpack.

Reference A.1 states that the storage overpack (HI-STORM 100) system was checked for a constant wind speed of 579 km/h (360 mi/h), a pressure drop of 20.7 kPa (3.0 psi) and three tornado-generated missiles. The three missiles are the same as the Spectrum I missiles identified in Reference A.18 and are characterized as follows:

(1) Automobile with a mass of 1,800 kg (3,970 lb) and a velocity of 203 km/h (126 mi/h)

(2) Rigid solid steel cylinder having a diameter of 20.3 cm (8 inches) with a mass of 125 kg (276 lb) and a velocity of 203 km/h (126 mi/h)

(3) Solid sphere having a diameter of 2.5 cm (1 inches) with a mass of 0.22 kg (0.49 lb) and a velocity of 203 km/h (126 mi/h)

The analysis in Reference A.1 demonstrates that the combination of the large tornado missile (automobile) plus either steady tornado wind or instantaneous pressure drop causes a maximum horizontal excursion of the storage cask midpoint (approximately equal to the cask center of gravity) of less than 14 cm (5.5 inches) or 2.7 degrees rotation. In order for the storage cask to tip-over, Reference A.1 reports the centroid must undergo a horizontal displacement of 168 cm (5.5 ft). Therefore, the storage cask will not tip-over due to the automobile impact. Furthermore, it is shown in Reference A.1 that the other two postulated missiles will not penetrate the storage overpack. The Spectrum II missiles in Reference A.18 are characterized in Table A.10.

Table A.10. Characteristics of Spectrum II Missiles

Missile	Mass (kg)	Dimensions (m)	Velocity m/s (mi/h)
(A) Wood Plank	52	0.092 x .289 x 3.66	83 (186)
(B) 6” Sch 40 pipe	130	0.168D x 4.58	52 (116)
(C) 1” Steel rod	4	0.0254D x 0.915	51 (114)
(D) Utility pole	510	0.343D x 10.68	55 (123)
(E) 12” Sch 40 pipe	340	0.32D x 4.58	47 (105)
(F) Automobile	1810	5 x 2 x 1.3	59 (132)

A.4.9.4.1 Automobile as Tornado Missile

The Spectrum II automobile has about the same mass as the Spectrum I automobile and the velocity is only slightly higher, i.e., 212 km/h versus 203 km/h (132 mi/h versus 126 mi/h). Therefore, the Spectrum II automobile missile when combined with the tornado wind or pressure drop will not cause the storage cask to tip-over.

The Reference A.1 report does not provide an evaluation of the potential for the storage cask to slide due to the combined effects of an automobile impact and tornado wind. The potential for this effect was evaluated in this Appendix. The Principle of Conservation of Momentum was used to calculate the initial velocity of the storage cask due to the impact of the automobile. The initial velocity of the storage cask was determined to be 2.33 km/h (1.45 mi/h). The force due to tornado wind effects was taken from Reference A.1 which showed that the force due to pressure drop governed over the tornado wind pressure.

The equation of motion for the struck storage cask is:

$$\frac{W}{g} x'' + \mu W - F_{Tornado} = 0 \qquad (A.24)$$

where: W = weight of storage cask
$F_{Tornado}$ = force due to tornado wind effect

Solving for x" results in the accelerations shown in Table A.11 for the range of coefficient of friction.

Table A.11. Acceleration for Range of μ

Coefficient of Friction (**μ**)	Acceleration(g)
minimum	0.005
mean	-0.18
maximum	-0.28

For a coefficient of friction of $\mu_{min} = 0.25$, the storage cask will have a positive acceleration of 0.005 g. This means that the storage cask will accelerate and continue to displace without stopping until it slides off the pad or hits another storage cask. For a coefficient of friction greater than 0.255, the storage cask acceleration is negative which means it will decelerate until it stops.

A.4.9.4.2 Other Spectrum II Tornado Missiles

The potential for the other Spectrum II missiles to penetrate the storage overpack was evaluated using the procedures given in Reference A.19 on pages C-6 through C-9. The penetration depth (x) is given as:

$$x = \left[4 K N W D \left(\frac{V}{1000 D} \right)^{1.8} \right]^{0.5} \quad \text{if } \frac{x}{D} < 2 \qquad (A.25)$$

$$x = K N W D \left(\frac{V}{1000 D} \right)^{1.8} + D \quad \text{if } \frac{x}{D} > 2 \qquad (A.26)$$

where: x = penetration depth (in)
K = concrete penetrability factor = $180/(f'_c)^{0.5} = 2.846$
N = shape factor = 0.72 for blunt missile
W = weight of missile
V = velocity of missile in ft/sec
D = diameter of missile (in)

When the missile first strikes the target, there is a tendency for the front face of the concrete to scab. The barrier thickness (t_{ds}) required to prevent this is given as:

$$t_{ds} = 1.1\left(2.12\,D + 1.36\,x\right) \qquad \text{for } 0.65 < x/D < 11.75 \qquad (A.27)$$

$$t_{ds} = 1.1\left(7.91x - 5.06\frac{x^2}{D}\right) \qquad \text{for } x/D < 0.65 \qquad (A.28)$$

If this scabbing thickness is not satisfied the penetration depths are likely to be larger than computed with Equations A.25 and A.26. Note that the 1.1 factors in Equations A.27 and A.28 are safety factors added to curve fits of empirical data. Of course, the outer steel plate on the storage overpack prevents this scabbing and is therefore not considered in this analysis.

The barrier thickness required to prevent the missile from perforating the shield (t_{dp}) is then given by:

$$t_{dp} = 1.2\left(1.32\,D + 1.24\,x\right) \qquad \text{for } 1.35 < x/D < 13.5 \qquad (A.29)$$

$$t_{dp} = 1.2\left(3.19x - \frac{0.718x^2}{D}\right) \qquad \text{for } x/D < 1.35 \qquad (A.30)$$

These calculations are conservative for the storage overpack for several reasons.

- The wall of the storage overpack includes inner and outer steel plates with the concrete contained within the plates. The above analysis includes only the effects of the concrete barrier so that lower penetration depths would be expected in the actual storage overpack.

- The above analysis was developed from data collected for plane barriers. The circular shape of the storage overpack would increase its strength as compared with a plane structure.

- The circular shape of the outer boundary of the storage overpack will tend to deflect missiles and thereby reduce the probability that a missile can penetrate the barrier.

The above calculations are carried out for the Spectrum II missiles. All of the missiles are included except for the automobile which was treated separately as discussed above because it is a large flexible missile and is more likely to cause gross response (sliding or tip-over) of the storage cask rather than to penetrate the storage overpack. The results of the calculations are shown in Table A.12.

The barrier thickness required to prevent penetration is less than the 68 cm (26.75 inches) of concrete provided except for the 12" Sch. 40 pipe where 72 cm (28.5 inches) is predicted as the thickness required to prevent penetration. Because of the conservatism cited above it is not likely that any of the missiles will penetrate the storage overpack.

Table A.12. Penetration of Missiles Through Reinforced Concrete Wall of Storage Overpack

Missile	f'c (psi)	K	N	Missile Weight (kg)	(lb)	Missile Velocity (m/s)	(ft/s)	Missile Diameter (cm)	(in)	V/1000D **1.8	x (in)	x/D	Req'd t (in)
Wood Plank	4000	2.846	0.72	52	114.64	83	272.3	18.4	7.244	0.00272	4.31	0.59	14.3
6" Sch 40 pipe	4000	2.846	0.72	130	286.6	52	170.6	16.8	6.614	0.00138	4.64	0.70	14.9
1" Steel Rod	4000	2.846	0.72	4	8.82	51	167.3	2.54	1.000	0.04003	1.70	1.70	4.1
Utility Pole	4000	2.846	0.72	510	1124.3	55	180.4	34.3	13.504	0.00042	7.26	0.54	26.6
12"Sch 40 pipe	4000	2.846	0.72	340	749.56	47	154.2	32.0	12.598	0.00036	5.29	0.42	28.5

Note: 1 inch = 2.54 cm; 1 psi = 6.895 kPa

A.4.9.5 Flood Water/Debris Impact Analysis

This calculation considers whether the effects of heavy objects in flood waters will cause the storage cask to slide and/or tip-over.

The subject plant FSAR states that none of the safety-related facilities would be exposed to river flooding by the most severe flood at the site. It is further reported that the probable maximum discharge concurrent with a severe wind of 72 km /h (45 mi/h) would develop a wave height of 2.5 m (6.5 ft). The elevation of the wave crest due to a sustained wind of this magnitude occurring during the Probable Maximum Flood would be well below the elevation of the top of the dry cask storage pad. Thus it would be an incredible event for flood waters to even reach the bottom of the storage cask and even more incredible for the storage cask to be impacted by heavy objects in flood waters.

The Reference A.1 report demonstrates that the accident condition design external pressure of 414 kPa (60 psi) for the MPC bounds the maximum hydrostatic pressure on the storage cask in a flood where the water level is conservatively set at 38 m (125 ft). The Reference A.1 report also evaluated the factor of safety against tip-over and sliding for a design basis flood velocity of 4.6 m/s (15 ft/s). They calculated a sliding factor of safety of 2.09 and a tip-over factor of safety of 4.68.

A calculation is performed to evaluate what forces/conditions due to floating debris would cause the storage cask to slide and/or tip-over. For this calculation, a floating tree moving at varying velocities is considered. The mass of the tree was approximated as three times the weight of the Spectrum II utility pole which results in a total weight of 1,530 kg (3,370 lb) that is close to the weight of the automobile. Conservatively, the location of impact was assumed to occur at the top of the storage cask.

The drag force due to the flowing flood water was also included for the same varying velocities as used for the debris impact. The velocities considered are 1.5 m/s (5 ft/s) , 3.0 m/s (10 ft/s), 6.1 m/s (20 ft/s), and 9.1 m/s (30 ft/s).

A.4.9.5.1 Tip-over Evaluation

The same methodology developed for the aircraft impact tip-over analysis was utilized (with an additional term for the constant water drag force). In this calculation, the kinetic energy due to impact and drag force

was compared to the potential energy required to cause tip-over. This comparison led to the conclusion that for velocities less than approximately 10.7 m/s (35 ft/s), the storage cask will not tip-over. The calculation also concluded that the contribution of the debris impact is negligible and can be dropped from the flood analysis of the storage cask. This occurred because the mass of the debris is a very small fraction of the storage cask mass and it is traveling at a very slow velocity.

A.4.9.5.2 Sliding Evaluation

Sliding would occur if the horizontal drag force is greater than the frictional resistance (the effect of debris impact can be neglected - see above). The calculation demonstrates that for velocities less than approximately 7.6 m (25 ft/s), the storage cask will not slide for the entire range of coefficients of friction. For velocities greater than that, the storage cask will slide depending on the velocity and the specific coefficient of friction. As an example, for a velocity of flowing water at 9.1 m (30 ft/s), the storage cask will slide for $\mu_{min} = 0.25$ but will not slide for $\mu_{mean} = 0.43$ and $\mu_{max} = 0.53$.

A.4.9.5.3 Analysis for Floods

An analysis for floods was performed with the following assumptions:

- Surface area of the storage cask subject to floods is 231.25 x 132.5 / 144 = 212.78 ft^2 or 19.8 m^2.
- Storage cask is rigid.
- Storage overpack has ventilation openings so it is assumed that the hydrostatic pressure from flood submergence acts only on the MPC.
- Water flow velocity is assumed to be uniform over the height of the storage overpack.
- C_d , the drag coefficient is 0.5.
- ρ, the water weight density is assumed to be 1,000 kg/m^3 (62.4 lbs/ft^3).
- μ, the coefficient of friction between steel plate and concrete pad is assumed to be 0.25.
  K_{min}, the buoyancy factor = 0.64 (Reference A.1)

<u>Sliding Evaluation</u>

Applied Force (lbs) $= C_d \cdot$ Velocity head $\cdot$ Area
$= 0.5 \times (\rho(lb/ft^{3)} \cdot V(ft/s)^2 / 2\, g(ft/s^2) \times 212.78ft^2 = 106.39\, (62.4\, V^2 / (2 \times 32.2))$
$= 103.09\, V^2$ (where V is in ft/sec; g is in ft/sec^2)

Resisting Force $= \mu \cdot K \cdot W$ (lbs)

where: μ = coefficient of friction
K = buoyancy
W = weight (lbs)
= 0.25 x 0.64 x W
= 0.16 W

For equilibrium, $103.09\, V^2 = 0.16\, W$

$V^2 = 0.001552\ W$
$V = (0.001552\ W)^{1/2}$ (ft/sec)

For overpack with minimum MPC Weight (lbs) $V = (0.001552 \times 303000)^{1/2} = 21.7$ ft/s (6.6 m/s)
For overpack with full MPC Weight $V = (0.001552 \times 360000)^{1/2} = 23.6$ ft/s (7.2 m/s)

Tip-over Evaluation

Applied Force (lbs) = $103.09\ V^2$ (where V is in ft/sec)

Applied Moment = Force · Height of A.G.
= $103.09\ V^2 \times (118.46$ inches$)/12$ inches/foot
= $1018\ V^2$ lb-ft

Resisting Moment = K · W · Diameter / 2 where W is weight
= $0.64 \times (132.5/24)\ W$
= $3.533\ W$

For equilibrium, $1018\ V^2 = 3.533\ W$
$V^2 = 0.00347\ W$ (lbs)
V (ft/sec) $= (0.00347\ W\ (\text{lbs}))^{1/2}$

For overpack with minimum MPC Weight (lbs) $V = (0.00347 \times 303000)^{1/2} = 32.4$ ft/s (9.9 m/s)
For overpack with full MPC Weight (lbs) $V = (0.00347 \times 360000)^{1/2} = 35.3$ ft/s (10.8 m/s)

To summarize, the flood required to slide the storage cask is at least 23.6 ft/s (7.2m/s), and the flood required to tip-over the storage cask is at least 35.3 ft/s (10.8 m/s).

A.4.9.6 Analysis for High Winds

An analysis for high winds (tornado) was performed with the following assumptions:

- Storage cask is assumed to be subjected to a constant wind force for full height.
- Storage cask is assumed to be rigid.
- μ, the coefficient of friction between steel plate and concrete pad is assumed to be 0.25.
- Storage cask is assumed to pivot about a fixed point at the outer edge of the contact surface.
- Surface area of the storage cask subject to wind = 231.25 x 132.5 / 144 = 212.78 ft^2 or 19.8 m^2
- C_d , the drag coefficient = 1.0

Sliding Evaluation

Applied Force (lbs) = C_d · Velocity head · Area
= $1.0 \times (\rho \cdot V^2 / 2g) \times$ Area Where ρ = air density = 0.07651 lb/ft^3 @ 15°C;
V is in ft/sec; g is in ft/sec^2

$= 0.07651 / (2 \times 32.2) \times V^2 \times$ Area
$= 0.00119 \times (5280/3600)^2 \times V^2 \times$ Area Where V is converted to mi/h
$= 0.00256 \times V^2 \times$ Area
$= 0.00256 \times 212.78 \times V^2$
$= 0.5447\ V^2$

Resisting Force $= \mu \cdot W$ where μ is coefficient of friction; W is weight (lbs)
$= 0.25$ W (lbs)

For equilibrium, $0.5447\ V^2 = 0.25\ W$
$V^2 = 0.459\ W$
$V\ (mi/hr) = (0.459\ W)^{1/2}$

For overpack with minimum MPC Weight (lbs) $V = (0.459 \times 303000)^{1/2} = 373$ mi/h or 600 km/h
For overpack with full MPC Weight (lbs) $V = (0.459 \times 360000)^{1/2} = 406$ mi/h or 653 km/h

<u>Tip-over Evaluation</u>

Applied Force $= 0.5447\ V^2$ Where V = wind in mi/h

Applied Moment = Force · Height of A.G.
$= 0.5447\ V^2 \times 118.46/12$
$= 5.377\ V^2$ lb-ft

Resisting Moment = W · Diameter / 2 where W is weight
$= (132.5/24)\ W = 5.52$ W lb-ft

For equilibrium, $5.377\ V^2 = 5.52\ W$
$V^2 = 1.02675\ W$
$V = (1.02678\ W)^{1/2}$

For overpack with minimum MPC Weight $V = (1.02675 \times 303000)^{1/2} = 558$ mi/h (898 km/h)
For overpack with full MPC Weight $V = (1.02675 \times 360000)^{1/2} = 608$ mi/h (978 km/h)

To summarize, the wind speed required to slide the storage cask is at least 653 km/hr (406 mi/hr), and the wind speed required to tip-over the storage cask is at least 978 km/hr (608 mi/hr). The design wind speed for the plant is 580 km/hr (360 mph).

A.4.10 Question 10

If the storage cask tips over on the concrete pad, what would be the stresses in the MPC?

To calculate accurate stresses in the MPC would require more than simplified analytical methods. Since the Reference A.1 report has already performed refined analyses, often using detailed finite element models, it would be best to utilize their results and scale the stresses to suit the scenario/case being evaluated. Therefore, the stress results from the Reference A.1 report will be used to tabulate the stresses in the MPC due to the tip-over case as well as the vertical "end drop" case. The end drop case is also included in this calculation because other calculations refer to this calculation to respond to some of the other questions. For example, stresses in the MPC due to transfer cask drop (Questions 3 & 4) refer to this calculation for a more complete listing of stresses.

For each type of loading, the acceleration and stresses are provided. If another calculation refer to this calculation for stresses, then the stresses presented herein should be scaled by the ratio of accelerations ($A_{New\ Ques.}/A_{Ques.\ 10}$). Scaling these stresses to higher acceleration values determined in other calculations is conservative.

Stresses in the MPC are provided for the fuel basket, basket supports, MPC shell, lid, and baseplate based on Reference A.1, Tables 3.4.3, 3.4.4, and 3.4.6. Maximum stresses are presented for the end drop case and the tip-over case for the MPC components listed above. The acceleration values corresponding to these stresses are also provided to permit scaling if needed in other calculations. For the tip-over case, two orientations of the basket walls with respect to the ground were considered, 0 degree and 45 degrees. The stresses and corresponding accelerations are summarized in the Table A.6.

A.4.10.1 Non-mechanistic Tip-over

Non-mechanistic tip-over refers to the case where the storage cask tips over due to the center of gravity of the cask passing over the point of rotation without any initial force or velocity. This case is non-mechanistic because there is no design basis type loading that would cause the cask to tip-over. It is presented to have a sense of what could be expected from a scenario that causes storage cask to be tilted to the point where it tips over. The maximum stress in the MPC, from Table A.6 for the tip-over case, is 406.5 MPa (58,959 psi). This is based on the Reference A.1 report which calculated the stress in the MPC shell using a finite element model of a slice of the MPC and fuel baskets subjected to an acceleration of 45 g. Under this loading, the MPC and fuel baskets deform outward until portions of the MPC shell reach the rigid boundary of the storage overpack inner steel shell. This analysis is considered conservative because it is based on a linear elastic approach. This stress of 406.5 MPa (58,959 psi) needs to be multiplied by a dynamic load factor of 1.04. Before applying the dynamic load factor, stresses due to internal pressure of 0.69 MPa (100 psi) must be removed, and then added after applying the dynamic load factor.

Stress due to 689 kPa (100 psi) internal pressure for the MPC shell thickness of 1.27 cm (0.5 inch) and an average diameter of 1.74 m (68.375 inches or 5.7 ft) is calculated by $p \cdot r / t = (100 \cdot 68.375/0.5)/0.5 =$ 6,838 psi or 47.1 MPa.

Stress in the MPC for tip-over = $(58959-6838) \cdot 1.04 + 6838 = 61{,}044$ psi or 421 MPa

So, the maximum circumferential stress in the MPC shell is approximately 421 MPa (61,044 psi) at 4.53 m (178.5 inches or 14.9 ft) above the bottom of the MPC. The maximum calculated stress is less than the allowable stress intensity of 450 MPa (65,200 psi) under Level D Service Condition of the ASME Code. Therefore, it does not cause the failure of the MPC.

The stress intensity of the MPC shell at the junction with the baseplate is the combination of stress due to internal pressure and the stress due to g value caused by tip-over. The stress intensity due to internal pressure of 0.69 MPa (100 psi), is 303 MPa (43,986 psi), based on the finite element analysis from Reference A.13. The stress intensity due to the tip-over is negligible at the MPC shell junction with the baseplate.

The total stress intensity at that junction is nearly the same as the stress caused by the internal pressure alone, which is less than the allowable stress intensity for Level D Service Condition of the ASME Code. Therefore, it does not cause the failure of the MPC.

If the storage cask tips over on another storage cask or on the ISFSI pad, calculations demonstrate that the studs retaining the lid on the overpack will resist the impact loads. In addition, the struck cask(s) will not tip-over.

A.4.11 Question 11

If the storage cask tips over, will the impact of the cask tipping over on another storage cask or on the concrete pad cause the overpack lid to be dislodged such that the MPC could slide out?

The bounding case is when the storage cask falls onto the concrete pad because this causes a larger acceleration. An analysis of the overpack lid integrity has already been performed by Reference A.1, Section 3.4.4.3.2.2, Appendix 3.K, and Appendix 3.L. Section 3.4.4.3.2.2 of Reference A.1 provides a summary of the overpack lid evaluation. Reference A.1, Appendix 3.K provides the stress analysis of the overpack lid. The Reference A.1, Appendix 3.L provides the calculation that demonstrates that the 4 studs hold the lid in place. For the reader's benefit the relevant portions of Appendix 3.K and Appendix 3.L are reproduced below:

A.4.11.1 Appendix 3.K - Lid Stress Analysis

Appendix 3.K describes the analysis of the lid due to the tip-over of the storage cask. It states that the maximum acceleration at the top of the overpack lid is 49 g as determined in Reference A.1, Appendix 3.A. Using the 49 g loading, the following lid components were checked in Reference A.1:

1. Lid Top Plate Stress Analysis (Plate Bearing Stress at Bolt Holes)
2. Lid Shell-To-Lid Top Plate Weld
3. Shield Block Shells-To-Lid Top Plate Weld
4. Lid Shell Stress Evaluation

Reference A.1, Section 3.4.4.3.2.2 summarizes the limiting stress of the lid to be:

τ = 61.6 MPa (8,940 psi)
τ (allowable) = 202.7 MPa (29,400 psi)
F actor of Safety = 3.29

A.4.11.2 Appendix 3.L - HI-STORM Lid Top Plate Bolting

The Appendix 3.L calculation shows that the four studs of 8.9 cm (3.5 inches) diameter holding the lid in place have sufficient strength. The calculation uses 48.5 g acceleration due to the tip-over based on Reference A.1, Table 3.A.4. Using a weight of 10,433 kg (23,000) lb for the lid times 48.5 g divided by the four studs result in a shear load on each stud equal to 126,099 (278,000 lb). This results in a shear stress of:

τ (bolt) = 231.8 MPa (33,620 psi) per bolt
τ (allowable) = (min. of $.42S_u$ or $.6\ S_y$) = 420 MPa (60,900 psi)
Factor of Safety = 1.81

Appendix 3.L also calculated the tensile stress due to (1) bending of the stud due to the lateral load acting on the stud over the thickness of the lid plate and (2) the pre-load of 407 N·m (300 lb-ft). The total tensile stress was calculated to be:

σ = 98,260 (bending) + 1,124 (pre-load) = 99,384 psi (685 MPa)
σ (allowable) = S_u = 1000 MPa (145,000 psi)
Factor of Safety = 1.46

Appendix 3.L then calculated the combined effect of tension and shear using an interaction equation which resulted in a factor of safety of 1.29.

It appears that the Reference A.1 report did not consider the effect of centrifugal force due to rotation of the storage cask. The centrifugal force would cause the MPC to push against the overpack lid imposing loads on the lid and studs. To determine the significance of this, the tensile stress on the studs due to centrifugal force was evaluated. The stress was calculated to be:

σ (centrifugal force) =19.7 MPa (2,857 psi)

This stress would not be in addition to the pre-load but in-place of the pre-load because this load would relieve the pre-load. Considering tension only and re-calculating the factor of safety, it reduces from 1.46 to 1.43 (a very small reduction). Considering shear and tension interaction, the factor of safety also shows a slight reduction from 1.29 to 1.26.

Based on the above discussion, it can be concluded that the overpack lid and studs are structurally adequate to resist the loads due to a tip-over of the storage cask, and thereby will prevent the MPC from sliding out of the storage cask.

A.4.12 Question 12

The shock waves from explosion that should be evaluated are those generated from: (1) an explosion from a typical tanker trailer containing explosive materials (gasoline, liquid/natural gas) at a distance of 914 m (3,000 ft) from the storage cask, and (2) an explosion of a natural gas pipeline at 7.2 km (4.5 mi) from the storage cask. Would the structural integrity of the cask system be in jeopardy if the shock waves caused by the postulated explosions are applied? If not, provide the supporting arguments.

Event A - Tanker Trailer at 914 m (3,000 ft)

Evaluation of Event A was conducted utilizing Reference A.22. Using the recommended Trinitrotoluene (TNT) equivalence factor of 240% and 22,680 kg (50,000 lb) cargo weight, the effective TNT weight is 54,431 kg (120,000 lb). From Equation (1) of Reference A.22, the peak transient pressure would be 1 psi at 677 m (2,220 ft). At 914 m (3,000 ft), the peak pressure would be less than 6.9 kPa (1 psi). The HI-STORM 100 cask (storage cask) is designed for a 69 kPa (10 psi) peak transient external pressure. Therefore, at 914 m (3,000 ft), the peak pressure due to the explosion would be less than 1/10 the pressure magnitude that the storage overpack is designed for.

Event B - Pipeline at 7.2 km (4.5 mi)

Evaluation of Event B was conducted utilizing References A.22 and A.23, which developed the probability of exceeding 3 psi external overpressure on the containment building of a proposed plant from a 21" ID pipeline containing methane at 4.9 MPa (720 psi) at a distance of 808 m (2,650 ft). The best estimate annual probability of exceedance was 6.0×10^{-7}/yr. Considering uncertainties, the range was 3.8×10^{-8}/yr to 2.3×10^{-6}/yr. Considering the higher allowable external pressure 69 kPa (10 psi) versus 21 kPa (3 psi), the much greater distance of 7.2 km (4.5 mi) versus 0.8 km (0.5 mi), and the smaller pipe ID (12" versus 21") for the present case, the annual probability of accedence should be significantly lower, perhaps by two to three orders of magnitude.

Reference A.22 does not address pipelines because of uncertainty associated with the formation of combustible gas clouds. However, for comparison to Event A, the equivalent of 6 river vessels

(27,215,542 kg (60,000,000 lb cargo)) simultaneously exploding at 7.2 km (4.5 mi) would produce a transient pressure of 6.9 kPa (1 psi) on the storage cask, based on Equation 1 of Reference A.22.

A.5 Conclusions

The events analyzed for the transfer cask are presented in response to Question 1 through 4. The conclusion reached from the analyses is that the strains in the MPC shell are well below the failure strain of the material. The MPC may yield and undergo some plastic deformation depending on the drop height, however, the MPC shell is not expected to rupture.

The event of MPC transfer from the transfer overpack to the storage overpack is addressed in response to Question 5. The results of the analysis demonstrate that the strains in the MPC are well below the failure strain of the shell material. The probability of the MPC shell rupture is discussed in Appendix B.

The events analyzed for the storage cask are presented in response to Questions 6 through 12. The analyses demonstrate that the storage cask will not slide significantly nor tip-over. For the Gulfstream IV impact analysis (Question 9) this conclusion is valid for an aircraft velocity less that 250 mph assuming worst case impact parameters. Furthermore, there will be no penetration of the storage overpack due to the Gulfstream IV impact or tornado missiles.

References

1. NRC Docket No. 72-1014, "Topical Safety Analysis Report for the Holtec International Storage and Transfer Operation Reinforced Concrete Module Cask System (HI-STORM 100 Cask System)," Holtec Report HI-951312, Volumes I and II, Revision 8, June 25, 1999.

2. LS-DYNA Computer Code and associated manuals, Version 960, March 2001, Livermore Software Technology Corporation.

3. American Concrete Institute, "Code Requirements for Nuclear Safety Related Concrete Structures (ACI 349)."

4. LS-DYNA Manual, Version 970, rev. 3858, LSTC, April 2003.

5. ASME Code, Section III, 1989, American Society of Mechanical Engineers.

6. Holt, J., Mindlin, H., O. C, Structural Alloys Handbook, CINDAS/Purdue University Press, 1996.

7. NRC Docket No. 72-1014. "HI-STORM Final Safety Analysis Report," Holtec International Report HI-2002444, Revision 0.

8. DOE Fundamentals Handbook, Material Science, Volume 2 of 2, DOE-HDBK-1017/2-93, January 1993, U.S. Department of Energy, Washington, D.C.

9. LLNL report, Dynamic Impact Effects on Spent Fuel Assemblies, by Ramsey Chun et. al., Lawrence Livermore National Laboratory, Livermore, California, October 1987.

10. TrueGrid Manual, Version 2.1.0, XYZ Scientific Applications, Inc., September 7, 2001.

11. NUREG/CR-6608, Summary and Evaluation of Low-Velocity Impact Tests of Solid Steel Billet Onto Concrete Pads, by LLNL, February 1998.

12. U. S. Nuclear Regulatory Commission, Certificate of Compliance No. 1014, Appendix B, "Approved Contents and Designed features for the HI-STORM 100 Cask System."

13. Cook, R. and Klingner, R., "Behavior of Ductile Multiple-Anchor Steel to Concrete Connections with Surface Mounted Base Plates," ACI Publication SP-130, 1999.

14. ABAQUS/Explicit: User's Manual, Version 5.8-19, 1998, Pawtucket, RI, Hibbitt, Karlsson, and Sorensen, Inc.

15. Idriss, I. M. and Seed, H. B., "Seismic Response of Horizontal Layers," Journal of the Soil Mechanics and Foundation Division, ASCE, Vol. 94, No. SM 4, July 1968.

16. Schnabel, P. B., Lysmer, J., and Seed H. B., "SHAKE: A computer Program for Earthquake Response Analysis of Horizontally Layered Sites," Report No. UCB/EERC-72/12, Earthquake Engineering Research Center, University of California, Berkeley, December 1972, 102p.

17. US Army Corps of Engineers, Engineer Technical Letter No. 1110-2-339, March 1993.January 8, 2003.

18. U. S. Nuclear Regulatory Commission, NUREG-0800, "Standard Review Plan," Section 3.5.1.4, "Missiles Generated by Natural Phenomena," Rev. 2, July 1981.

19. DOE Standard 3014-96, "Accident Analysis for Aircraft Crash into Hazardous Facilities," October 1996.

20. U. S. Nuclear Regulatory Commission, NUREG/CR-5042, "Evaluation of External Hazards to Nuclear Power Plants in the United States," December, 1987.

21. NRC Docket No. 72-1008. "HI-STAR 100 Final Safety Analysis Report," Holtec Report HI-2012610, Rev. 0.

22. U. S. Nuclear Regulatory Commission, Regulatory Guide 1.91, "Evaluation of Explosions Postulated to Occur on Transportation Routes Near Nuclear Power Plants," Revision 1, February 1978 (For Comment).

23. Mechanics Research Inc. Report No. MRI-2687-75, "Nuclear Power Plant Risks from a Natural Gas Pipeline," dated August 2, 1974, prepared for TVA, Knoxville TN.

24. Braverman, J. I., Nie, J., Morante, R. J., Simos, N., Hofmayer, C. H., "Accidental Drop Analyses of a Spent Fuel Dry Cask System," Brookhaven National Laboratory, BNL-Y6423-032905, March 2005.

25. Bjorkman, G. S., "The Buckling of Fuel Rods in Transportation Casks under Hypothetical Accident Conditions," Proceedings of PATAM 2004, Berlin, Germany, 2004.

26. US Nuclear Regulatory Commission (USNRC), "Buckling of Irradiated Fuel under Bottom End Drop Conditions," ISG-12, Revision 1, 1999.